HHS Public Access

Author manuscript

Cell Rep. Author manuscript; available in PMC 2022 March 26.

Published in final edited form as:

Cell Rep. 2022 March 08; 38(10): 110494. doi:10.1016/j.celrep.2022.110494.

Odorant-receptor-mediated regulation of chemosensory gene expression in the malaria mosquito *Anopheles gambiae*

Sarah E. Maguire[1,3], **Ali Afify**[1], **Loyal A. Goff**[1,2], **Christopher J. Potter**[1,4,*]

[1]Solomon H. Snyder Department of Neuroscience, Johns Hopkins University School of Medicine, Rangos 434, 855 N. Wolfe Street, Baltimore, MD 21205, USA

[2]Department of Genetic Medicine, Johns Hopkins University School of Medicine, Baltimore, MD 21205, USA

[3]Present address: Sanaria, 9800 Medical Center Drive, Suite A209, Rockville, MD 20850, USA

[4]Lead contact

SUMMARY

Mosquitoes locate and approach humans based on the activity of odorant receptors (ORs) expressed on olfactory receptor neurons (ORNs). Olfactogenetic experiments in *Anopheles gambiae* mosquitoes revealed that the ectopic expression of an *AgOR (AgOR2)* in ORNs dampened the activity of the expressing neuron. This contrasts with studies in *Drosophila melanogaster* in which the ectopic expression of non-native *ORs* in ORNs confers ectopic neuronal responses without interfering with native olfactory physiology. RNA-seq analyses comparing wild-type antennae to those ectopically expressing *AgOR2* in ORNs indicated that nearly all *AgOR* transcripts were significantly downregulated (except for *AgOR2*). Additional experiments suggest that AgOR2 protein rather than mRNA mediates this downregulation. Using *in situ* hybridization, we find that *AgOR* gene choice is active into adulthood and that AgOR2 expression inhibits *AgORs* from turning on at this late stage. Our study shows that the ORNs of *Anopheles* mosquitoes (in contrast to *Drosophila*) are sensitive to a currently unexplored mechanism of *AgOR* regulation.

Graphical Abstract

*Correspondence: cpotter@jhmi.edu.

AUTHOR CONTRIBUTIONS

S.E.M. and C.J.P. designed the research; S.E.M., A.A., and L.A.G. performed the research; S.E.M., A.A., and L.A.G. analyzed the data; and S.E.M. and C.J.P. wrote the paper.

DECLARATION OF INTERESTS

The authors declare no competing interests.

SUPPLEMENTAL INFORMATION

Supplemental information can be found online at https://doi.org/10.1016/j.celrep.2022.110494.

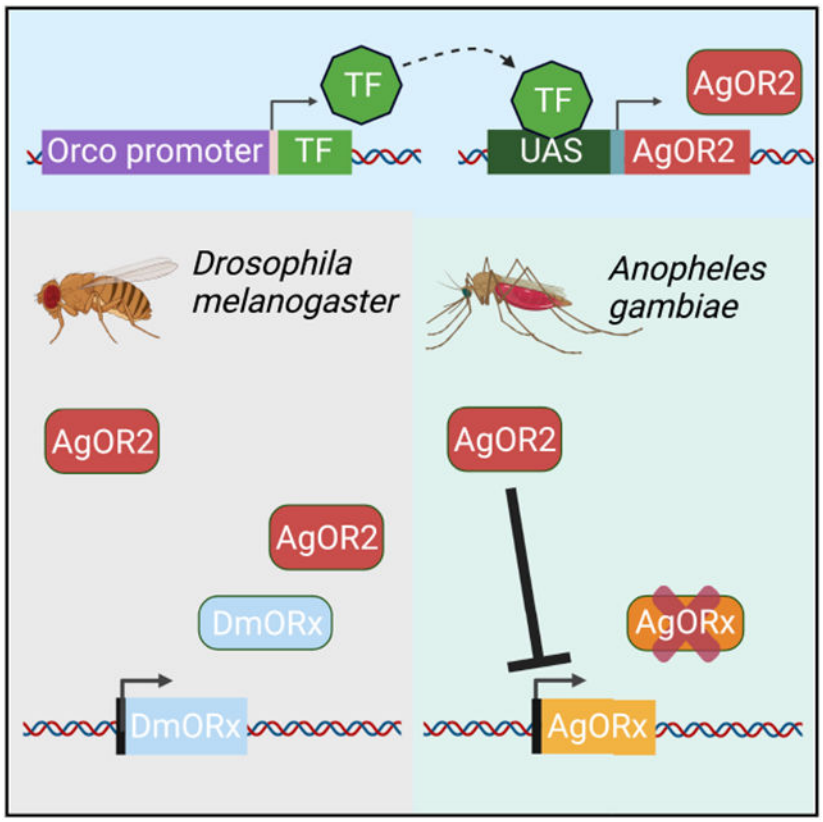

In brief

Maguire et al. discover that the ectopic expression of an olfactory receptor can downregulate the transcription of endogenous odorant receptors in mosquito olfactory neurons. The onset of mosquito odorant-receptor expression by an olfactory neuron continues into adult stages, and is particularly sensitive to exogenous olfactory reception expression.

INTRODUCTION

Malaria is a major cause of human mortality worldwide (Global Malaria Programme, 2019), and it is a global health imperative to prevent the spread of this disease. Malaria is caused by *Plasmodium* parasites transmitted by the bite of infected *Anopheles* mosquitoes. To date, antimalarial drugs have been the mainstay of control against malaria, and over the past 15 years, these treatments, along with the distribution of insecticide-treated bed nets, have contributed to an overall reduction of disease transmission. However, the eventual eradication of malaria likely rests on a multidisciplinary approach that integrates our knowledge of host, parasite, and vector biology (Cowman et al., 2016). For example, impairing the ability of the insect vector to bite a human host may further reduce incidences of infection. As such, disrupting the behaviors that bring mosquitoes to humans could dramatically reduce the prevalence of malaria (Beauty and Marquardt, 1996).

Female *Anopheles* mosquitoes locate and approach humans (“host seek”) based on specific cues, such as human-derived odors and exhaled CO_2, moisture and heat emissions, and body

shape (Konopka et al., 2021). The primary way that mosquitoes host seek is through their sense of smell (olfaction). Mosquitoes have evolved a complex repertoire of chemoreceptors that respond to chemical stimuli such as ionotropic receptors (IRs), gustatory receptors (GRs), and the odorant receptors (ORs). Of these, the ORs play a substantial role in mediating how a mosquito responds to human odors (DeGennaro et al., 2013). ORs form heterotetramer complexes with an OR co-receptor (ORCO) (Butterwick et al., 2018). OR-ORCO complexes are expressed on olfactory receptor neurons (ORNs) of the sensory appendages of the mosquito: antennae, maxillary palps, and labella (Riabinina et al., 2016). $ORCO^+$ ORNs are housed in "sensilla," or the sensory hairs of these appendages. Each sensillum typically contains 1–4 ORNs that each express a unique OR, of which there are 75 in the *A. gambiae* genome (Giraldo-Calderón et al., 2015). These ORNs are classified and named by the OR gene they express, and each $ORCO^+$ ORN class targets a specific brain region of the mosquito antennal lobe (AL) known as a glomerulus (Couto et al., 2005; Ghaninia et al., 2007). The decision to approach a host is a direct result of activated $ORCO^+$ ORNs targeting a specific combination of glomeruli (Figures 1A and 1B).

Disrupting this specificity by activating all $ORCO^+$ ORNs in the presence of human odors has been hypothesized to prevent host seeking (Clark and Ray, 2016; Jones et al., 2011). Studies in *Drosophila*, the insect model of olfaction, show that binary systems can be used to express non-native ORs in $ORCO^+$ ORNs to confer ectopic neuronal responses without interfering with native olfactory physiology. Therefore, we examined whether this strategy could be used to disrupt host seeking in *A. gambiae* mosquitoes. To test this, we expressed *A. gambiae OR 2 (AgOR2)* in all *ORCO*$^+$ ORNs. AgOR2 is highly attuned to major components of human and animal odors such as benzaldehyde and indole (Carey et al., 2010), and in the presence of human odors, all *ORCO*$^+$ neurons expressing AgOR2 should become active. Surprisingly, when we evaluated the olfactory physiology of these experimental mosquitoes, we found that they exhibited reduced responses not only to the cognate ligands of AgOR2 (benzaldehyde and indole) but also to odorants in general. To investigate the molecular basis of this phenotype, we looked for signatures of dysfunction at the level of the transcriptome. Using RNA sequencing (RNA-seq) to compare transcript levels from wild-type antennae to those ectopically expressing *AgOR2*, we discovered that *A. gambiae OR* isoforms were significantly downregulated in the experimental line, while the remaining transcripts were largely unchanged. Additional experiments revealed that AgOR2 protein rather than *AgOR2 mRNA* is needed to reduce native *OR* levels. We also made the unexpected finding that *AgOR* gene choice extends into adulthood—a stage in *Drosophila* when each ORN is thought to have already chosen a distinct *OR* (McLaughlin et al., 2021)—because AgOR2 suppresses an increase in *AgOR*-expressing cells observed in wild-type antenna 1–8 days post-eclosion (PE). Overall, our study suggests that an OR-mediated feedback mechanism exists that can regulate *A. gambiae OR* expression.

RESULTS

Ectopically expressing *AgOR2* in *ORCO*$^+$ neurons impairs olfactory physiology

To activate *ORCO*$^+$ ORNs in the presence of human odorants, we used olfactogenetics, a technique whereby a specific volatile odorant is used to activate a defined set of OR-

expressing neurons (Chin et al., 2018). To accomplish this, an *OR* with known response properties is ectopically expressed in ORNs of interest through the use of a binary expression system, such as the Q-system (Riabinina et al., 2015) or the GAL4-UAS system. Thus, in the presence of odorants in which the introduced OR normally responds, ORNs with ectopic expression become active.

The recent introduction of the Q-system into *Anopheles* makes it possible to adapt olfactogenetics in mosquitoes (Riabinina et al., 2016). As a binary expression system, the Q-system works by directing the expression of a specific gene into a specific cell population. This particular system relies on two elements: QF2 and *QUAS*. The QF2 transcription factor is expressed under the control of a cell-type-specific enhancer/promoter and binds to its upstream activating sequence, *QUAS*. Once bound by QF2, *QUAS* initiates the transcription of its effector gene. To ectopically activate $ORCO^{+}$ ORNs in the presence of human odors, we combined a mosquito line containing *ORCO-QF2* (Riabinina et al., 2016), which contains a fusion between the presumptive enhancer and promoter regions of the gene *ORCO* and the transcription factor QF2, with an effector line containing a *QUAS* transgene upstream of *A. gambiae OR 2, AgOR2 (QUAS-AgOR2)*. Thus, experimental animals exhibit the ectopic expression of *AgOR2* in all $ORCO^{+}$ ORNs (Figure 1C).

AgOR2 is highly attuned to components of human and animal odors such as benzaldehyde and indole (Carey et al., 2010), and it was expected that $ORCO^{+}$ ORNs of *ORCO >AgOR2* mosquitoes would become active in the presence of these cognate ligands, essentially activating the majority of the olfactory system during host seeking (Figure 1D). To test the functional activity of ORNs ectopically expressing *AgOR2* in mosquitoes, we imaged the calcium response of *ORCO > AgOR2* antennal segments in a *QUAS-GCaMP6f* background *(ORCO > AgOR2,GCaMP6f).* Surprisingly, *ORCO > AgOR2,GCaMP6f* antennae showed a dampened response not only to various concentrations of benzaldehyde and indole but also to odorants in general (Figure 2A). For example, octenol potentially activates 31 different *A. gambiae* ORs (Carey et al., 2010), but the ORNs of the experimental mosquitoes did not show a response to this odorant. In *Drosophila*, a single ORN class can drive behavior at spike rates as low as 10–20 Hz (Bell and Wilson, 2016). When we stimulated *ORCO > AgOR2,GCaMP6f* with 5 additional odorants known to activate 14–16 different ORN classes at rates higher than 50 spikes/s (Carey et al., 2010), the ORNs still did not exhibit odorant-induced responses (Figure S1).

One possibility for the observed olfactory defects (Figures 2A and S1) is that the *QUAS-AgOR2* transgene inserted into an endogenous olfactory gene and disrupted olfactory function. To date, the genome organization is unavailable for the *Anopheles* strain used in this study (*A. coluzzii N'gousso*, ACON), so we used splinkerette mapping (Potter and Luo, 2010) to align the insertion site of the *QUAS-AgOR2* element to a related *Anopheles* strain (*A. coluzzii Mali*, ACOM). The transgenic line examined in Figures 2A and S1 (line 1) is located in an intergenic region on chromosome 3R between the genes ACOM029303 and ACOM029196. While it is unlikely that this particular insertion site would disrupt the function of an olfactory gene necessary for ORN physiology, we extended our studies to analyze the physiology of two additional *QUAS-AgOR2* lines inserted into different regions of the genome. We established line *QUAS-AgOR2#2*, which maps to an intergenic region

between ACOM036217 and ACOM036230, and line *QUAS-AgOR2#3*, which could not be mapped by splinkerette PCR. When driven into *ORCO*$^{+}$ cells, all three lines show similar defects in olfactory physiology when compared to wild type (Figure S2). Furthermore, since these lines were tested as heterozygotes, any recessive mutation in an olfactory gene caused by the *QUAS-AgOR2* insertion should be compensated by the wild-type allele. Overall, these data show that the dominant-negative olfactory phenotype (Figures 2A, S1, and S2) is a consequence of ectopic *AgOR2* expression rather than the genomic insertion site of the *QUAS-AgOR2* element.

Olfactogenetics impairs *Anopheles* but not *Drosophila ORCO*$^{+}$ ORNs

Ectopically expressing an *OR* in *Drosophila* ORNs causes the expressing neuron to activate in the presence of the odor ligand of the introduced OR (Carey et al., 2010; Chin et al., 2018; Dobritsa et al., 2003; Hallem et al., 2004; Ray et al., 2007). One possibility as to why *ORCO > AgOR2* cells in the mosquito did not respond to benzaldehyde or indole was because the *AgOR2* sequence used to create the transgenic *QUAS-AgOR2* line was acting in a dominant-negative manner to disrupt ORCO/OR_X ion channels. To test this, we ectopically expressed *AgOR2* in *Drosophila ORCO*$^{+}$ neurons using the GAL4-UAS system and measured the response rate of neurons housed in the ab1 sensilla using single sensillum recordings (SSRs). Ab1 contains 4 ORNs, 3 of which are *ORCO*$^{+}$ and express *DmOR10a, DmOR42b*, and *DmOR92a*, and one of which is *ORCO*$^{-}$ and expresses the GR *DmGR21*, which responds to CO_2. To determine whether ectopic expression of *AgOR2* impairs native DmOR responses to their cognate ligands, responses of the DmOR10a-expressing neuron to methyl salicylate were measured. We found no difference in how control (*ORCO-GAL4*) and experimental *(ORCO > 5xAgOR2)* sensilla responded to methyl salicylate, indicating that *AgOR2* expression does not interfere with the olfactory physiology of the neuron in which it is expressed. Furthermore, native responses of DmOR10a were not affected when an even higher dosage of *AgOR2* was driven into the neuron (*ORCO > 20xAgOR2*) (Figure 2B). When we puffed benzaldehyde over the experimental preparation, *ORCO*$^{+}$ cells in the *Drosophila* ab1 sensilla ectopically responded. Interestingly, sensilla that have higher levels of ectopic *AgOR2* can still maintain ectopic responses without compromising neuron function. When we used the stronger effector line (*20XUAS*) to ectopically express *AgOR2* in *Drosophila ORCO*$^{+}$ neurons, the olfactogenetics approach continued to work and olfactory physiology was not impaired.

In *Drosophila*, the *DmORCO* gene turns on relatively late—80 h after puparium formation (APF) during the development of the adult olfactory system—and is approximately coincident with the onset and expression of *DmOR* genes (Clyne et al., 1999; Elmore et al., 2003; Larsson et al., 2004; Trebels et al., 2021). We next examined whether driving *AgOR2* expression earlier in development, before the onset of *DmOR* expression, would affect odorant responses. *Pebbled-Gal4* drives expression in most cells residing in the antenna and maxillary palp during development and can be observed as early as 18 h APF in ORNs (Sweeney et al., 2007), before the detection of the earliest expressing *DmOR* genes at 24 h APF (McLaughlin et al., 2021). Using *pebbled-Gal4* to ectopically drive *5xUAS-AgOR2* or *20xUAS-AgOR2* in ORNs, the DmOR10a-expressing neurons in ab1 sensilla continue to respond normally to methyl salicylate (Figure S3).

The *Anopheles* capitate peg (cp) sensillum is similar to the ab1 sensillum of *Drosophila* as it contains *ORCO*$^+$ ORNs, which express *AgOR8* and *AgOR28*, and one *ORCO*-independent ORN that responds to CO_2. When we ectopically expressed *AgOR2* in *ORCO*$^+$ ORNs in the mosquito and recorded from cp sensilla, we found that the response of the AgOR8-expressing neuron to octenol, its cognate ligand, was eliminated (Figure 2C). In addition, neither AgOR8 nor AgOR28-expressing neurons ectopically respond to benzaldehyde. Similar to *Drosophila*, the genetic manipulation does not affect the physiology of the *ORCO*$^-$ CO_2-responsive neuron (Figure 2C). These data indicate that olfactogenetics affects the physiology of *Drosophila* and *Anopheles ORCO*$^+$ ORNs differently: in flies, ectopically expressing *OR*s does not affect endogenous neuronal function, whereas in *Anopheles* mosquitoes, the ectopic expression of *AgOR2* disrupts the function of the ORNs.

Ectopic AgOR2 protein eliminates olfactory responses in *ORCO*$^+$ cells

It is possible that driving an *AgOR* into an *Anopheles* ORN is cytotoxic, especially if the neuron experiences continual stimulation from the environment. To assess whether *ORCO > AgOR2* mosquitoes show ORCO$^+$ cell loss, we (1) compared the number of ORCO$^+$ cells per flagellomere to that of the genetic control and also (2) evaluated whether *ORCO > AgOR2* ORN projections to the AL were intact. Using immunochemistry to visualize ORCO$^+$ cells in the periphery and ORN terminals in the AL, we found that ORN cell number and projections were unperturbed in *ORCO > AgOR2*, indicating that the lack of ORN responses to odors was not due to the death and elimination of neurons ectopically expressing *AgOR2* (Figure S4). Next, we tested whether driving any generic transmembrane protein into *Anopheles* ORNs also hindered olfactory physiology. To evaluate this, we used the *ORCO-QF2* driver to ectopically express the transmembrane protein *mCD8:GFP* into all *ORCO*$^+$ neurons. There were no differences in the odor-induced responses between control and *mCD8:GFP*$^+$ ORNs (Figure S5), suggesting that the ectopic expression of another transmembrane protein did not silence ORN activities.

Ectopic *AgOR2* expression may inhibit olfactory responses either at the level of *AgOR2* mRNA or at the level of AgOR2 protein. To distinguish between these two possibilities, we created a transgenic mosquito line containing a mutated version of *AgOR2 (mutAgOR2)* that contained a mutation in the start codon of *AgOR2* such that *QUAS-mutAgOR2* produced mRNA that cannot be translated when combined with *ORCO-QF2*. We also induced a frameshift mutation at a second in-frame ATG site in *mutAgOR2* to eliminate the possibility of having an alternative open reading frame used during translation. We crossed *QUAS-mutAgOr2* with *ORCO-QF2,QUAS-GCaMP6f* and found that the calcium responses were not compromised (Figure 3); only when the wild-type version of the protein was expressed (*QUAS-AgOR2*) was the odor response impaired (Figures 2A, 2C, S1, and S2). Taken together, these data suggest that the AgOR2 protein itself, and not mRNA, was responsible for the olfactory defect of *ORCO*$^+$ cells (but see limitations of the study in the discussion).

Ectopic AgOR2 reduces the transcripts of native *AgORs*

How might AgOR2 protein impair olfactory responses? We hypothesized this may occur as a result of (1) regulatory mechanisms affecting *AgOR* transcription, stability, and/or

degradation rates or (2) regulatory mechanisms and/or defects in AgOR protein function. These transcriptional or post-translational mechanisms may act together or independently. To distinguish between these two possibilities, we performed isoform-level RNA-seq on antennae isolated from control and *ORCO > AgOR2* samples. Of the ~13,000 transcript isoforms detected (Data S1), only 83 were differentially expressed in the *ORCO > AgOR2* mosquito antennae. Interestingly, half of these differentially expressed isoforms (41/83) were *AgORs*, all of which were downregulated in *ORCO > AgOR2* antennae, except for *AgOR2*, which was highly upregulated when compared to the wild type (Figures 4A and S6; Data S2). As shown by the *AgOR* isoform comparison heatmaps in Figure 4B, control *AgOR* levels are higher than those in *ORCO > AgOR2*, with the exception of *AgOR2*, which is upregulated.

If AgOR2 ectopic protein was responsible for modulating the steady-state abundance of native *AgOR* transcripts, then the relative abundance of the *A. gambiae OR* gene family isoforms in *ORCO > mutAgOR2* antennae should not be affected. To test this, we extracted biological triplicates of mosquito antennae from female mosquitoes of the *ORCO > mutAgOR2* line and compared the isoform abundance levels of this group to the original RNA-seq dataset. Ternary plots depicting the relative abundance of isoform expression levels in control, *ORCO > mutAgOR2*, and *ORCO > AgOR2* conditions as a position on an equilateral triangle were used to explore how *AgOR* and other gene sets were differentially expressed. To depict how control, *ORCO > mutAgOR2*, and *ORCO > AgOR2* contribute to relative isoform abundances of non-*AgOR* genes and *AgOR* genes, we created 2 discrete ternary plots. As expected, the relative contribution of control, *ORCO > mutAgOR2*, and *ORCO > AgOR2* for all non-*A. gambiae OR* isoforms in the transcriptome was roughly equal (34.3%:33%:32.6%). However, when removing the contribution of the ectopically induced *AgOR2* from the *AgOR* isoform pool, the relative contribution of the abundance levels of an *AgOR* was reduced in *ORCO > AgOR2* relative to control and *ORCO > mutAgOR2* groups: 45.8%:37.8%:16.4% (control:*ORCO > mutAgOR2:ORCO > AgOR2*) (Figure 4C). Results of the gene set enrichment test and pairwise comparisons of *AgOR* isoforms can be viewed in Figure S7. The majority of native *AgORs* are downregulated in *ORCO > AgOR2* but not in *ORCO > mutAgOR2*, with four exceptions: *AgOR2, AgOR16, AgOR17*, and *AgOR33*.

AgOR2 feedback occurs during the adult stage of the life cycle of the mosquito

We next examined when, during the life cycle of the mosquito, the downregulation of native *AgOR* transcripts occurred by ectopic AgOR2. Since ectopic AgOR2 expression is dictated by the *ORCO* enhancer/promoter region (Figure 1C) (Riabinina et al., 2016), AgOR2-induced olfactory silencing of native *AgOR* genes should coincide with the AgORCO expression pattern. Holometabolous insects, such as mosquitoes, experience four developmental stages during their lifespan: egg, larva, pupa, and adult stages. Since the lifestyle of adults and larvae differ, the olfactory system is remodeled to take on adult features during pupal development (Mysore et al., 2011, 2013; Trebels et al., 2021), so we performed immunohistochemistry on pupal antennae from *ORCO > mCD8:GFP* mosquitoes every 4 h starting at the onset of pupal development (0–2 h APF) to just before eclosion (20–22 h APF), which happens at 24 h APF. AgORCO (as reported by mCD8 staining) was

expressed immediately after pupal ecdysis at 0–2 h APF (Figures 5A and 5B). Interestingly, ORCO expression turned on gradually in antennal ORNs. Starting at 8–10 h APF (when the first antennal flagellomeres could be observed), each segment gained ~15 ORCO$^+$ cells every 4 h, starting from 37.5 ± 2 cells and ending with 87 ± 20 cells per flagellomere at 20–22 h APF (Figures 5A and 5B). These data suggest that the ectopic expression of AgOR2 in the *ORCO > AgOR2* genotype (which coincides with ORCO) also occurred throughout pupal development, and may impinge upon developmental mechanisms that regulate *AgOR* expression. To see whether this was the case, we used *in situ* hybridizations to characterize the expression patterns of the 3 *AgOR* genes most significantly downregulated by ectopic AgOR2: *AgOR11, AgOR24*, and *AgOR41* (Figure 4 and S7; Data S2). In wild-type ORNs, *AgOR11*$^+$, *AgOR24*$^+$, and *AgOR41*$^+$ cells were first detected at 8–10 h APF and continued to increase in number into adulthood up to the last time point sampled: 4–8 days PE (Figures 5C and 5D). This is well past what was typically considered the end of *OR* gene choice as determined by other insect model organisms of olfaction (Trebels et al., 2021). In *ORCO > AgOR2*-expressing mosquitoes, *AgOR11*$^+$, *AgOR24*$^+$ and *AgOR41*$^+$ cells were also observed starting at 8–10 h APF and showed no differences in number until 20–22 h APF. From 20 to 22 h APF until the last time point sampled (4–8 days PE), *AgOR11-, AgOR24-*, and *AgOR41*-expressing cells did not increase in number as they did in the wild type. We speculate that this may be because at these later stages, *AgOR2 mRNA* and AgOR2 protein is expressed in every ORN (Figures 5B and 5E) and would prevent ORNs that have not yet chosen an *AgOR* from expressing transcripts from the *AgOR* gene family. Overall, these data show that the negative inhibition of *AgOR* genes by AgOR2 protein occurs during the establishment of *AgOR* gene choice, which extends into adulthood.

Impairing *ORCO*$^+$ neuron responses inhibits olfactory preference but not host-seeking behavior in *Anopheles* mosquitoes

In the absence of CO_2, *ORCO* mutant *Aedes* (DeGennaro et al., 2013; Raji et al., 2019) and *Anopheles* (Sun et al., 2020) mosquitoes demonstrate reduced host attraction. Under conditions that replicate an environment containing a naturally breathing human, CO_2 synergizes with host odors to rescue defects in *ORCO* mutant attraction (DeGennaro et al., 2013), suggesting that mosquitoes possess redundant mechanisms (such as IR genes) that activate in the presence of CO_2 (Raji et al., 2019). The dominant-negative phenotype of *ORCO > AgOR2* presented the opportunity to test whether *Anopheles* mosquitoes with impaired ORCO function also continue to host seek in the presence of CO_2. To test this, we used the host-proximity assay (DeGennaro et al., 2013), a population assay that measures the proportion of females that come into olfactory (but not physical) contact with a human arm. As found with *ORCO* mutant *Aedes* mosquitoes (DeGennaro et al., 2013; Raji et al., 2019), *Anopheles* mosquitoes without functional *ORCO*$^+$ neurons were still attracted to a human host in the presence of CO_2 (Figures 6A-6C).

While *Anopheles* mosquitoes continue to show strong attraction to host odors in the presence of CO_2, it is likely that a loss of functional ORCO-expressing neurons impairs the ability of mosquitoes to discriminate between odorants (DeGennaro et al., 2013). Oviposition preference by gravid females is in part mediated by their olfactory system (Montell and Zwiebel, 2016). Sun et al. (2020) demonstrated that *Anopheles* mosquitoes

without ORCO function cannot discriminate between substrates emanating control versus attractive odors, but it is unknown whether defects in ORCO function also cause mosquitoes to become insensitive to repellent odors. Lemongrass oil is a known mosquito repellent that activates a subset of *ORCO*$^{+}$ ORNs (Afify et al., 2019). When we evaluated repellent odorant discrimination using an oviposition-based assay, we found that control genotypes laid fewer eggs on substrates emanating 0.1% lemongrass oil odor. In contrast, *ORCO > AgOR2* mosquitoes laid the same number of eggs on oviposition substrates emanating 0.1% lemongrass oil or control odorants, indicating that an impairment in ORCO function causes a mosquito to lose sensitivity to repellent odors (Figure 6D).

DISCUSSION

We report that a mechanism may exist to regulate *AgOR* gene stability in insects. A main finding of our study—that AgOR protein downregulates the expression of native *AgORs* (Figure 7)—is a pattern more closely resembling OR-regulatory processes in mice than those of *Drosophila*. This study demonstrates that driving ectopic expression of *AgOR2* in non-native *ORCO*$^{+}$ ORNs does not disrupt *Drosophila* neuron function, whereas in *Anopheles* it does (Figures 2 and S1-S3). Furthermore, ectopically expressing a *DmOR* gene in *Drosophila* ORNs does not affect the gene expression of native *DmORs* (Ray et al., 2007), whereas a similar manipulation in *Anopheles* leads to robust changes in gene expression (Figures 4 and S7; Data S2).

From these experiments, we hypothesize that unexpected similarities of *AgOR* gene regulation may exist between *Anopheles* and mice. For example, both *Anopheles* and mice contain a negative feedback loop by which OR protein inhibits the expression of the remaining *ORs*. In *Anopheles* mosquitoes, as was the case in mice, this feedback pathway likely requires intact OR protein (Figures 3 and 4; with 3 exceptions: see Figure S7) since expressing mutant *OR* genes lacking either the entire coding sequence or the start codon permits a second *OR* gene to be expressed (Feinstein et al., 2004; Lewcock and Reed, 2004; Serizawa et al., 2003; Shykind et al., 2004). Frameshift mutations also allow for the co-expression of functional *OR* genes (Serizawa et al., 2003). It remains to be determined whether mice and *Anopheles* mosquitoes use similar cellular machinery to regulate *OR* stability (Dalton et al., 2013).

Our data demonstrate that AgOR2 feedback occurs during the development of the olfactory system in *Anopheles* mosquitoes (Figure 5). Why might OR feedback be important for olfactory development? One consequence of OR feedback is that it increases the likelihood that a single ORN expresses only 1 OR, which is an important developmental mechanism in mice because ORs play an instructive role in guiding ORN axonal projections to the olfactory region of the brain (Mombaerts et al., 1996; Vassar et al., 1994; Wang et al., 1998). In experiments analogous to those presented here, when multiple ORs are genetically engineered to co-express in a single ORN in mice, the topographic map of projections to the olfactory center in the brain is perturbed (Clowney et al., 2012). While we do not know when ORNs target the AL in *Anopheles*, our methods expressed *AgOR2* in *ORCO*$^{+}$ neurons as early as 0–2 h APF (Figure 5). If ORNs have not yet targeted the AL at this early stage, then our data suggest that *AgORs* in *Anopheles* are likely not involved in axon guidance, as

we did not detect obvious deformations of ORN targeting or AL structure in the adult brain (Figure S4). Why else might AgOR feedback be important during olfactory development? OR feedback (at least in mice) serves to reduce the expression of the remaining *OR* genes in an ORN, ensuring the singular expression of an OR by stabilizing the gene choice. We show that *AgOR* gene choice in ORNs continues into the adult stage (Figures 5C and 5D), which is traditionally thought to end at the late pupal stage (McLaughlin et al., 2021; Trebels et al., 2021). It is an intriguing possibility that the process of *AgOR* gene choice and stabilization remains active during adult stages as a way to allow the mosquito to synergize the physiology of ORNs with biological needs. *Anopheles* mosquitoes rely heavily on their sense of olfaction to integrate ecologically relevant stimuli that change over the course of their adult lifespan. When females first eclose, they are uninterested in host odors (Omondi et al., 2019) and instead actively search for sugar-rich resources from plants to supplement their nutrient reserves. After a period of ~4 days PE, they develop an attraction to host odorants (Foster and Takken, 2004; Omondi et al., 2019) and following a blood meal will experience a refractory period to host odorants until after oviposition. These changes in behavior have been correlated with changes in chemosensory gene transcript abundance both in *Anopheles* (Omondi et al., 2019) and *Aedes aegypti* (Tallon et al., 2019). More recently, Hill et al. (2021) demonstrated that *Aedes aegypti* mosquitoes show age- and state-dependent regulation of *AeOR* gene expression during adulthood. It would be interesting to determine whether this dynamic regulation observed in bulk antennal tissue is a consequence of mosquito *OR* gene levels changing within their native cells or whether new *ORs* are being chosen and stabilized via OR feedback.

AgORs can be co-expressed within the same ORN when transcribed as polycistronic mRNA (Karner et al., 2015). Polycistronic *AgOR* mRNA is observed in cases when *AgOR* genes are clustered tightly together within the genome. Such clustering of *OR* genes is commonplace in mosquito species such as *A. gambiae* (Hill et al., 2002) and *Aedes aegypti* (Bohbot et al., 2007), as well as in mice (Sullivan et al., 1996; Zhang et al., 2004); however, to our knowledge, polycistronic *OR* mRNA has not been observed in rodent olfactory systems. It is possible that polycistronic *OR* expression avoids the negative feedback mechanism of *OR* regulation, enabling the neuron to co-express multiple *ORs*.

While ectopically expressing *AgOR2* downregulates native *AgOR* genes, it was surprising that *ORCO > AgOR2* neurons did not show responses to the cognate ligands of AgOR2 (benzaldehyde and indole). From our RNA expression data, we estimate that a single wild-type ORN contributes 0.006 transcripts per million (TPM) of a given *AgOR* to a single antennal sample (calculations in Data S3). We estimate that ectopically expressing *AgOR2* increases the *AgOR* expression level of a single cell to 0.02 TPM (2.5×). If all of the expressed *AgORs* are being translated in a cell, this would elevate the amount of AgOR protein that is normally observed in wild-type ORNs. We hypothesize that elevated AgOR protein levels impair olfactory physiology by disrupting the stoichiometry of the AgOR-ORCO complexes, rendering them non-functional. While research has shown that AgORs form stable heteromeric complexes with AgORCO (Benton et al., 2006; German et al., 2013; Neuhaus et al., 2005; Tsitoura et al., 2010), the stoichiometry underlying AgOR-ORCO channels is unknown. RNA-seq data from this study (Data S3) and from two independent studies (Athrey et al., 2017; Pitts et al., 2011) show that in wild-type conditions,

there is a conserved ~1:1 relationship between total *AgOR* transcripts and *AgORCO* in bulk antennal tissue. Interestingly, we see that ectopic *AgOR2* expression does not change *AgORCO* expression (Figure 4B), skewing the estimated ratio of *AgORs:AgORCO* in a single cell from 1.2:1 in wild-type to 3:1 in *ORCO > AgOR2* (Data S3). Since ORCO is required to traffic OR:ORCO complexes to the dendritic surfaces (Benton et al., 2006), increasing AgOR2 expression may interfere with this process. Alternatively, changes to the OR:ORCO stoichiometry may result in a functional defect in the channel itself, whereby the malformed complexes cannot respond to odors even if they have been successfully trafficked to the membrane. Finally, mosquito-specific defects caused by the ectopic expression of AgOR2 may depend on its partnering with AgORCO, which was not present in the *Drosophila* experiments. Future studies will be required to examine these possibilities.

This study adds to the mounting evidence that the disruption of a single sensory modality is insufficient to eliminate host-seeking behavior toward a naturally breathing host. As first demonstrated in *Aedes aegypti*, mosquitoes with a mutation in the *ORCO* gene remain attracted to humans in the presence of CO_2 (DeGennaro et al., 2013); under these conditions, we also find that *Anopheles* mosquitoes with impaired ORCO neuronal function continue to host seek (Figures 6A-6C). In addition to odors, mosquitos are attracted to a wide variety of human-derived cues, including heat, CO_2, visual stimuli, and moisture, and so one sensory modality is likely able to compensate for the loss of another (DeGennaro et al., 2013; Greppi et al., 2020; McMeniman et al., 2014; Raji et al., 2019). While the loss of ORCO function does not impair host-seeking behavior in the presence of CO_2, Sun et al., 2020 (Sun et al., 2020) demonstrated that *Anopheles ORCO* mutant mosquitoes lose their preference for attractive odorants. Interestingly, loss of ORCO function also prevents *Anopheles* mosquitoes from discriminating between repellent and control odorants (Figure 6D). These data have important consequences for vector control strategies aimed at manipulating ORCO function, as mosquitoes defective in $ORCO^+$ ORN activities will not only continue to host-seek but may also have reduced sensitivity to select repellents.

Limitations of the study

Our study uncovers the existence of a mechanism of *AgOR* regulation in insects whereby ectopic expression of an AgOR results in the downregulation of other native *AgOR* gene isoforms (Figure 4). A major limitation of this study is that only a single insect OR was examined in *Anopheles* mosquitoes. It remains to be determined whether ectopic expression of other insect ORs besides AgOR2, such as *Drosophila* ORs or other mosquito ORs, can similarly trigger *AgOR*-expression regulation or whether the effects observed are specific to *AgOR2*. In addition, the mutations introduced to eliminate AgOR2 protein expression while retaining mRNA levels (*mutAgOR2*; data shown in Figures 3 and 4) may trigger nonsense-mediated decay; this could reduce *mutAgOR2* abundance. Finally, while *Anopheles* mosquito olfactory neurons are affected by ectopic *AgOR2* expression, it remains to be determined to what extent this mechanism is used during normal olfactory neuron development. Nonetheless, this work lays the technical and conceptual foundations to explore cellular mechanisms used by mosquito ORNs to regulate *AgOR* expression.

STAR★METHODS

RESOURCE AVAILABILITY

Lead contact—Further information and requests for resources and reagents should be directed to and will be fulfilled by the lead contact, Christopher J. Potter (cpotter@jhmi.edu).

Materials availability—All unique/stable reagents generated in this study are available from the lead contact with a completed Materials Transfer Agreement.

Data and code availability

- Raw and analyzed RNA-seq datafiles generated during this study have been deposited on NCBI (dataview.ncbi.nlm.nih.gov/) and are publicly available as of the date of publication. The BioProject accession number is listed on the key resources table. All data reported in this paper will be shared by the lead contact upon request.
- This paper does not report any original code.
- Any additional information required to reanalyze the data reported in this paper is available from the lead contact upon request.

EXPERIMENTAL MODEL AND SUBJECT DETAILS

Anopheles gambiae M-form strain Ngousso (the M-form of *An. gambiae* is now referred to as *Anopheles coluzzii*) were grown at 28°C, 70-75% relative humidity and 14hr light/10hr dark cycle. Larvae were reared at low densities (175 larvae/1L dH_2O) to ensure large adult size. They were provided with TetraMin Tropical Flakes and Purina Cat Chow Indoor pellets *ad libitum*. Pupae were hand collected and allowed to eclose in small cages, where they were provided with 10% sucrose continuously. Almost all pupae eclosed the day after collection. Adult males and females were kept together in the same cage for 7-10 days, after which they were fed mouse blood from anaesthetized mice according to Johns Hopkins University Animal Care and Use Committee (ACUC) approved protocol #M019M483. Eggs were collected from the resulting gravid females by providing them with a cup of water containing wet filter paper on which to deposit their eggs as an oviposition substrate. Each generation was screened for the presence of the eye specific marker encoded by the inserted plasmid cassette.

Drosophila melanogaster: Flies were reared at 25°C and 70% humidity on a standard cornmeal diet.

METHOD DETAILS

Insect stocks—*Mosquitoes: ORCO-QF2* and *QUAS-mCD8::GFP* transgenic mosquito stocks were generated as described in Riabinina et al. 2016 (Riabinina et al., 2016). *QUAS-GCaMP6f* was generated as described in Afify et al. 2019 (Afify et al., 2019). Wild-type Ngousso mosquitoes were a gift from the Insect Transformation Facility (Rockville, MD). *D. melanogaster: ORCO-GAL4; P{Orco-GAL4.W} 11.17* (BDSC: 26818),

5xUAS-AgOR2; w[*];Df(2L)dp-79b Dp(2;2)dpp[d21]/cyo;P{w[+mC]=UAS-Agam\Or2}3/TM3,Sb[1] (BDSC: 58828), and *Pebbled-GAL4; w[*]P{w[+m*]=GAL4}peb* (BDSC: 80570) lines were obtained from the Bloomington *Drosophila* Stock Center.

Recombinant DNA construction—Plasmids were constructed by enzyme digestions, PCR, subcloning and the In-Fusion HD Cloning System (Clontech, 639645). Plasmid inserts were verified by restriction enzyme digests and DNA sequencing. Insertions of each plasmid into the *Anopheles* genome (*QUAS-AgOR2, QUAS-mutAgOR2*) or the *Drosophila* genome (*20xUAS-AgOR2*) were verified by sequencing the vector-specific cassette within the transgenic animal. To create the *pXL-BacII-15xQUAS-TATA-AgOR2-Sv40* plasmid, we linearized the *pXL-BacII-15xQUAS_TATA-Sv40* (Riabinina et al., 2016) vector with *XhoI*. The cDNA of *AgOR2* was amplified from Bloomington Drosophila Stock Center 58828 using the oligos *Aga_OR2_F* (5′-ATTCGTTAACAGATCTATGCTGATCGAAGAGTGTCCGA-3′) and *Aga_OR2_R* (5′-CCTTCACAAAGATCGACGTCTTAGTTGTACACTCGGCGCAGC-3′). The resultant PCR product was then infusion-subcloned back into the construct. To create the *pXL-BacII-15xQUAS-TATA-mutAgOR2-Sv40* reporter line, a double digest of *pXL-BacII-15xQUAS-TATA-AgOR2-Sv40* with *BgIII* and *XhoI* was performed. *AgOR2* was amplified from *pXL-BacII-15xQUAS-TATA-AgOr2-Sv40* using a forward primer that mutated the start codon: ATG→TTT (*InfuMUTAgOr2_for*: 5′-ATTCGTTAACA GATCTTTTCTGATCGAAGAGTGTCCGATAATTG-3′). The reverse primer was engineered to create a frameshift mutation at a second in-frame ATG site located between the first and second transmembrane domains of *AgOR2* (*InfuMUTAGOr2_rev*: 5′- CGT CATTTTTCTCGAGTAGAGAGCGTACTCGGCGGC-3′). The *pJFRC-20xUAS-AgOR2* reporter was created in *Drosophila* to test whether increasing the dosage of *AgOR2* affects olfactory physiology. The construct was made by digesting *pJFRC-20xUAS-IVS-CD8GFP* (Pfeiffer et al., 2010) with *NotI* and *XbaI* and isolating the linearized 8.1kb vector. *AgOR2* was PCR amplified from *pXL-BacII-15xQUAS-TATA-AgOR2-Sv40* using the primers *UAS-AgOr2-FOR* (5′-TTACTTCAGGCGGCC GCAAA ATGCTGATC GAAGAGTGTCCG-3′) and *UAS-AgOR2-REV* (5′-ACAAAGATCCTCTAGA TTAGTTGTACACTCGGCGCAG-3′). The PCR product was infusion cloned into the digested *pJFRC-20xUAS* vector. Upon sequence confirmation, the plasmid was isolated using a Midiprep kit (Qiagen 12145) and sent to Rainbow Transgenics (rainbowgene.com) for injection into the attP2 site (RFT # 8622). The *pXL-BACII-DsRed-OR7_9kbProm-QF2-hsp70* construct was used to generate the *ORCO-QF2* driver line in this study. Construction of this plasmid is described in Riabinina et al. 2016 (Riabinina et al., 2016). All plasmids were constructed using MacVector v17.0.10 (MacVector, Inc.; Macvector.com).

Anopheles gambiae* transgenics—Anopheles gambiae* M-form strain Ngousso (the M-form of *An. gambiae* is now referred to as *Anopheles coluzzii*) mosquitoes were grown at 28°C, 70-75% relative humidity, 12h light/dark cycle. Freshly deposited eggs were collected by providing mated, gravid females with wet filter paper as an oviposition substrate for 15-20min, after which the eggs were collected and systematically arranged side-by-side on a double-sided tape fixed to a coverslip. Aligned embryos were covered with halocarbon

oil and injected at their posterior pole with an injection cocktail between 30-40min after egg laying. Injection cocktails consisted of a mixture of two plasmids, one with a piggyBac vector carrying the transgene of interest with a dominant visible marker gene – enhanced cyan fluorescent protein (ECFP) – under the regulatory control of the *3xP3* promoter, and a piggyBac transposase-expressing plasmid consisting of the transposase open reading frame under the regulatory control of the promoter from the *An. stephensi vasa* gene. Vector concentrations were at 150 ng/uL and the transposase-expressing plasmid was at 300 ng/uL in 5mM potassium chloride, 0.1mM sodium phosphate pH 6.8. Halocarbon oil was immediately removed and coverslips with injected embryos were placed in trays of water at 28°C, where the first instar larvae hatched ~24hr later. The Insect Transformation Facility (https://www.ibbr.umd.edu/facilities/itf) within the University of Maryland College Park's Institute for Bioscience and Biotechnology Research performed all embryo microinjections. Adults developing from injected embryos were separated by sex at the pupal stage before mating, and small groups of 5-10 injected adult males or females were crossed to wild-type Ngousso adults of the opposite sex. The progeny from these matings were screened during the third or fourth larval instar for the presence of vector-specific marker gene expression. Transgenic larvae were saved and adults from these larvae were outcrossed to wild-type for a total of 5 generations.

Calcium imaging—Preparation: *In vivo* preparation of mosquitoes (ages 3-10 days) and optical imaging of odor-evoked calcium responses are described in Afify et al. 2019 (Afify et al., 2019). *Genotyping mosquitoes*: After the recordings were made for each sample, the bodies of all mosquitoes were frozen for subsequent genomic DNA extraction and genotyping. At the time of the experiment, our transgenic lines were not homozygous. Because all *QUAS* effector lines (*QUAS-AgOR2, QUAS-mutAgOR2, QUAS-GCaMP6f*) are marked with the dominant eye marker, ECFP, we had to determine – for each sample – whether the mosquito contained a single copy of *QUAS-AgOR2*, a single copy of *QUAS-GCaMP6f*, or both *QUAS-AgOR2* and *QUAS-GCaMP6f* transgenes (for experiments in Figures 2A, S1, and S2). For the experiment in Figure 3, we had to determine – for each sample – whether the mosquito contained a single copy of *QUAS-mutAgOR2*, a single copy of *QUAS-GCaMP6f*, or both *QUAS-mutAgOR2* and *QUAS-GCaMP6f* transgenes. To genotype *QUAS-GCaMP6f*, we used the primers *gcamp6f_for2* (5′-ATGGTATGGCTAGCATGACTG-3′) and *gcamp6f_rev* (5′- GTAGTTTACCT GACCATCCCC-3′). Females that did not have any amplification of *GCaMP6f* were discarded from the analysis. To genotype *QUAS-AgOR2* or *QUAS-mutAgOR2*, we used the following primers: *AgOr2_for1* (5′- TAATTGGTGTCAATGTGCGAG-3′) and *AgOr2_rev2* (5′- TTATCGGCTCCTCAAAGTCTG-3′). The PCR was designed so that both the wild-type *AgOR2* (1542bp) and the transgenic *AgOR2* (966bp) (or *mutAgOR2*; 968bp) – if present – would amplify. For each female, we determined whether she contained the wild-type and transgenic copy of *AgOR2* (or *mutAgOR2*) or only the wild-type *AgOR2*. Scoring of all calcium imaging files was done blind to genotype. *Analysis*: To make the heatmaps (ΔF), Fiji software (Schindelin et al., 2012) was used with a custom-built macro. This Macro uses the "Image stabilizer" plug-in to correct for movements in the recording, followed by the "Z project" function to calculate the mean baseline fluorescence (mean intensity in the first 9s of recording, before stimulus delivery). The "Image calculator" function was used

to subtract the mean baseline fluorescence from the image of maximum fluorescence after odorant delivery (this image was manually chosen). Afterward, this ΔF image was used to produce heatmaps. To quantify the ΔF value for each segment to each odorant, the "ROI manager" tool in Fiji was used to manually select an ROI. For each sample, we manually drew the 'antennal ROI' around the 11th antennal segment from an epifluorescent image taken for each sample prior to the calcium imaging. We also drew a 'background ROI' outside of the tissue using the same surface area as the 'antennal ROI' to control for any background signal. A "task manager" was used to store the location of the antennal ROI and the background, and the mean intensity across the antennal segment (or background control) for each odorant was stored for each ROI. The final ΔF value was taken for each antennal segment and each odorant as the mean intensity of the 'antennal ROI' minus the 'background ROI.' Of note, the imaging software was upgraded for Figure 3, which explains why the (ΔF) values in Figure 3 are on a different scale than Figures 2A, S1, and S2. Data were analyzed using JMP Version 9, SAS Institute Inc.; jmp.com.

SSR—*Drosophila* preparation. Flies were housed on standard food in groups of a maximum of 10. Analysis was done on ab1 sensilla from 6-10 day old male flies. Sensilla of targeted ORNs were prepared and identified using methods described in Lin & Potter 2015 (Lin and Potter, 2015). Briefly, ab1 sensilla were identified by their response to CO_2. Ab1 is the only sensillar group that houses the CO_2-responsive neuron, and so a CO_2-response was indicative that the sensillum recording from was ab1. Signals were amplified 100X (USB-IDAC System; Syntech, Hilversum, The Netherlands), inputted into a computer via a 16-bit analog-digital converter and analyzed off-line with AUTOSPIKE software (USB-IDAC System; Syntech; ockenfels-syntech.com). The low cutoff filter setting was 50Hz, and the high cutoff was 5kHz. To deliver odorants or CO_2 to ab1, a constant air stream was guided through a serological pipette with a tip placed 1cm from the antenna. The chemical cartridge was laterally inserted into this airflow. Stimuli consisted of 1000ms air pulses passed over odorant sources, which were various odorants diluted in paraffin oil (30μL on a filter paper of 1x2cm). For the benzaldehyde (Millipore Sigma, B1334; CAS: 100-52-7) analysis, every spike was counted (neuron subtypes were not distinguished). For the methyl salicylate (Millipore Sigma, M6752; CAS:119-36-8) analysis, only responses from the DmOR10a-positive neuron were included. Delta spikes/second were calculated by manually counting the number of spikes in a 0.5s window at stimulus delivery (200ms after stimulus onset to account for the delay due to the air path) and then subtracting the number of spontaneous spikes in a 0.5s window before stimulation, multiplied by 2 to obtain delta spikes per second. *Mosquito preparation*. Mated females were 5-12 days old and not bloodfed. Extracellular recordings of the cps on the maxillary palps were made using the same equipment as for *Drosophila* SSR (see above). Cp sensilla were also identified by their response to CO_2. Cp is the only sensillum that houses the CO_2-responsive neuron, and so a CO_2-response was indicative that the sensillum we were recording from was cp. SSR data were analyzed using JMP Version 9, SAS Institute Inc.; jmp.com.

RNA-seq—To generate experimental pools of *ORCO>AgOR2* antennae, mosquitoes of the genotype *QUAS-AgOR2* were crossed to *ORCO-QF2*. Simultaneously, we generated control samples by crossing *ORCO>AgOR2* or *ORCO-QF2* strains to wild-type (2 crosses).

All 3 crosses were conducted in large breeding cages that consisted of ~75 males and ~75 females. Crosses were blood-fed a total of 4 times and progeny from each cross were screened for the eye-specific fluorescent markers. Larvae generated from experimental crosses were screened for the presence of ECFP and DsRed, markers for the *QUAS* and the *ORCO-QF2* transgenes, respectively. Larvae that did not contain both markers were discarded. For the control larvae progeny, animals that contained a single eye marker (either DsRed or ECFP, respectively) were kept in control pools that consisted either of *ORCO-QF2* or *QUAS-AgOR2* alone. All mosquitoes used in this study were heterozygous for a given transgene. *ORCO>mutAgOR2* and *QUAS-mutAgOR2* library preparations were made using the procedure described above with the exception that the antennae were extracted at a different time. To prepare antennal RNA-seq libraries, we isolated RNA from approximately 200 antennae from age-matched cohorts (11 total samples: 3 experimental samples containing *ORCO>AgOR2* antennae (*ORCO-QF2 + QUAS-AgOR2*), 5 control samples consisting of 2 samples from *ORCO-QF2* antennae, 2 samples from *QUAS-AgOR2* antennae, and 1 sample from *QUAS-mutAgOR2* antennae, and 3 experimental samples containing *ORCO>mutAgOR2* antennae). These mated females were within their fertile period (5-20 days old) and did not receive a bloodmeal. To create the antennal RNA-seq libraries, we removed the whole antenna from the base of the pedicel and isolated total RNA using TriZol purification methods. The tissues were disrupted and homogenized using a power pestle with disposable RNase free pestles. Total RNA samples were stored at −80°C and shipped to Genewiz, Inc. (genewiz.com), where they were first assessed for quantity (Qubit Quantification) and quality (Agilent 2100 Bioanalyzer). RNA library preparation with polyA selection was then carried out using the *Illumina* HiSeq with a 2x150bp configuration. Paired end reads were pseudoaligned to the AgamP4.12 reference transcriptome (Giraldo-Calderón et al., 2015) and isoform-level abundances were quantified using kallisto v0.46.0 (Bray et al., 2016) using default parameters with the following exceptions: −t4 and −bl00. Per-sample abundances were aggregated and normalized in R (R Core Team, 2018) using sleuth v0.30.0 (Pimentel et al., 2017). For each pairwise comparison (AgOR2 v control, mutAgOR2 v control, and mutAgOR2 v AgOR2), we fit a full sleuth model using condition as an explanatory variable. Differentially expressed isoforms were identified using the Wald test ($q \leq 0.01$, Benjamini-Hochberg corrected) for each model fit. Ternary plots were constructed using the ggtern R package (Hamilton and Ferry, 2018). Gene ontology (GO) annotations for the differentially expressed isoforms were assigned by Vectorbase.org (Giraldo-Calderón et al., 2015). Raw and analyzed RNA-seq data were deposited on NCBI, BioProject: PRJNA771697.

Immunohistochemistry—*Adult Antennae*: Antennae of 5+ day old *ORCO>AgOR2* and *QUAS-AgOR2* were extracted and stained as described in Basrur et al. 2020 (Basrur et al., 2020), with one exception. Female heads were incubated for 1 hour 20 minutes in chitinase-chymotrypsin solution before fixation and subsequent antennal removal. Mouse anti-*Apocrypta bakeri* ORCO monoclonal antibody #15B2 (Butterwick et al., 2018) (1:50 dilution, gift of Joel Butterwick and Vanessa Ruta) was used to visualize ORCO-positive cells. *Brains*: Brains of female mosquitoes of *ORCO>mCD8::GFP* and *ORCO>AgOR2,mCD8::GFP* genotypes were extracted and stained as described previously (Riabinina et al., 2016). Once genotyped via a PCR designed to amplify the transgenic

and wild-type copies of *AgOR2* (see 'calcium imaging section' above), experimental and control brains were separated and stained in two different groups. Rat anti-CD8 (Invitrogen Cat#MCD0800, 1:100) was used to visualize the ORN projections to the ALs and mouse nc82 (Developmental Studies Hybridoma Bank, 1:50) was added to visualize the structure of the brain. *Pupal Antennae: ORCO>mCD8::GFP* larvae were collected in 2 trays, each of which contained ~60 larvae. At the given timepoint APF, the cephalothorax and abdomen of the pupae were extracted and the antennae, oculus, compound eye, and rudimentary appendages were placed in 4% paraformaldehyde (PFA) with 0.1% triton phosphate buffer solution (PBS-T). Antennae were then dissected out and washed 3x in 1X PBS-T (0.1%). Antennae were then blocked for 30min at 4°C with 5% normal goat serum (NGS). To visualize mCD8::GFP expression, we added rat anti-CD8(Invitrogen, Cat#MCD0800, 1:100), which was left to incubate on a rotator overnight at 4°C. The next day, antennae were washed 3x in 1X PBS-T (0.1%) and Alexa-488 goat anti-rat (Invitrogen Cat#A110066, 1:200) was added to the solution. After 1.5hr at 25°C, antennae were washed 2X in 1X PBS-T (0.1%) and the last wash in 1xPBS to remove the triton. Antennae were placed on slides and mounted in SlowFade Gold Antifade Mountant.

Whole mount antennal RNA *in situ* hybridization—RNA was detected in whole mount antennae using the hybridization chain reaction (HCR) technique as described in (Younger et al., 2020) with few modifications. Probes were designed against *AgOR2, AgOR11, AgOR24*, and *AgOR41*. The 488 and 546 amplifiers, probe hybridization buffer, amplification buffer, and probe wash buffer were purchased from Molecular Instruments (molecularinstruments.com/). *AgOR11, AgOR24*, and *AgOR41* probes were designed to be conjugated with Alexa 488 and probes for *AgOR2* were designed to be conjugated with Alexa 546. Heads from female wild-type and *ORCO>AgOR2* pupae (0-2hr APF, 4-6hr APF, 8-10hr APF, 12-14hr APF, 16-18hr APF, and 20-22hr APF) and adults (1 day PE, 4-8 days PE) were digested in a chitinase-chymotrypsin solution for 25 minutes and fixed overnight at 4°C. The following day, the heads were dehydrated with a graded series of methanol/ 0.1% PBS-Tween-10 at 4°C. Tissues were incubated in 100% methanol for 2-3 days and were subsequently rehydrated with a series of graded methanol/0.1% PBS-Tween-20 at 4°C. Heads were then washed in 0.1% PBS-Tween-20 and pupal or adult antennae were dissected. Adult (but not pupal) antennae were digested in 20 ug/mL Recombinant Proteinase-K Solution in 0.1% PBS-Tween for 30 minutes at room temperature, washed in 0.1% PBS-Tween-20, and fixed in 4% paraformaldehyde in 0.1% PBS-Tween-20 for 20 minutes and then washed 3x in 0.1% PBS-Tween-20. Probe hybridization, wash, and amplification steps were then followed as described in Younger et al. 2020 (Younger et al., 2020).

Confocal imaging and analyses—Brains and antennae were imaged on an LSM 700 Zeiss confocal microscope with a 40x immersion-corrected objective at a resolution of 512x512 pixel resolution with 0.9uM Z-steps. For illustration purposes, confocal images were processed using Fiji (Schindelin et al., 2012) to collapse the maximum intensity projection of Z-stacks into a single image. For the immunohistochemistry experiment, we used cells that were immunoreactive to mCD8 as a proxy for ORCO expression. Cells per flagellomere were counted manually in pupal and adult antennae.

Host-proximity assay—The design and methods of the host-proximity assay are modified from DeGennaro et al. 2013 (DeGennaro et al., 2013). Briefly, for each trial, 20-30 adult female *Anopheles* mosquitoes (5+ days PE, mated but not blood-fed) were sorted under cold anesthesia (4°C), placed in 24-oz deli containers (https://www.amazon.com/gp/product/B00NB9WCEO/ref=oh_aui_detailpage_o06_s00?ie=UTF8&psc=1), and fasted with access to water for 16-24hr prior to assaying. Pre-fasting and behavior experiments took place at 27°C and 70-80% relative humidity. Experiments took placed after zeitgeber time 0 (ZT0) and continued until ZT8. 5 minutes before the start of the assay, mosquitoes were released into a modified BugDorm (https://shop.bugdorm.com/bugdorm-1-insect-rearing-cage-p-1.html). After 5 minutes had elapsed, pure CO_2 and synthetic air (air flow rate: 0.1L/min, CO_2 flowrate 145MM) were mixed in an adaptor before being pulsed (3 sec on: 3 sec off) into a flypad (8.1 x 11.6 cm catalogue #59-114; Flystuff.com, San Diego, CA), which was placed at the bottom of the BugDorm. Mosquitoes were then presented with a single volunteer's arm, which was placed 2.5 cm away from one side of the BugDorm so that mosquitoes could not come into direct contact with the arm. To control the distance from the arm to the cage, a Q-Snap needlework frame (https://www.amazon.com/dp/B00013MV30/ref=twister_B07CQQJKL2?_encoding=UTF8&psc=1) was placed flush against the cage and the arm was pressed against the vials. The arm was elevated 2.7 cm by placing it on a plastic microcentrifuge test-tube rack. An HDR-CX260V camera (Sony) was positioned to take images of mosquitoes responding to the human arm. Trials ran for 3 minutes. To quantify mosquito responses that came into 'close proximity' to the human arm, we counted the number of mosquitoes resting on the screen. We did not include mosquitoes that had landed on the white area surrounding the screen nor the mosquitoes that were in flight. For the % attraction figure, we scored the number of mosquitoes that came into close proximity of the arm every 10 seconds from minute 1 to minute 3 and then divided this number by the total number of mosquitoes in the trial. Data were analyzed using JMP Version 9, SAS Institute Inc.; jmp.com.

Olfactory-based oviposition preference assay—Olfactory-based oviposition preference was evaluated in groups of 10, 10-12 day old gravid females for the following genotypes: wild-type, *ORCO-QF2, QUAS-AgOR2*, and *ORCO>AgOR2*. Three days prior to preference assay, blood-fed females were placed in aluminum mosquito cages (BioQuip, Cat#1450A) and allowed to acclimate to a 12L:12D light:dark cycle maintained at 27°C, 75% RH. On day four, control (paraffin oil) and repellent (0.1% lemongrass oil (Millipore Sigma; W262440; CAS:8007-02-01; diluted in paraffin oil) 'double cups' (Mwingira et al., 2019) were placed in opposite corners of the cage. Double cups separate the influence of physical and olfactory cues on oviposition site selection by gravid females. A double cup consists of a small cup (4.3 cm top diameter x 2.9 cm bottom diameter x 3.2 cm height) filled with 10 mL of deionized water placed inside a larger cup (5.7 cm top diameter x 3.8 cm bottom diameter x 6.3 cm height) filled with 1 mL control or repellent solution. To induce egg laying, filter paper, a mosquito oviposition substrate, was placed in the small cup and left for 24 hrs. The small cup prevented contamination of the filter paper with the control or repellent solution. The following day, the number of eggs laid on the control and repellent double cup filter papers were scored manually for each genotype. Egg laying for each genotype was assessed over the course of 7 trials for each genotype and the position

of control and repellent double cups were randomized across all trials. For each genotype, a paired-samples t-test was used to assess if there were differences in egg number between the control and repellent double cups. Statistical analyses were performed in R (R Core Team, 2018).

QUANTIFICATION AND STATISTICAL ANALYSIS

Information regarding the quantification and statistical analyses performed on all data are described in the method details section or in the figure legends. All statistical tests were run in JMP Version 9 (SAS Institute, Inc.; jmp.com) or R (R Core Team, 2018; r-project.org).

Supplementary Material

Refer to Web version on PubMed Central for supplementary material.

ACKNOWLEDGMENTS

This research benefited from the limitless enthusiasm and support of Potter Lab members, both past and present. In particular, we would like to thank Kateline Robinson Shaw and Liz Marr for assisting with molecular biology. Darya Task and Joanna Konopka helped rear the transgenic mosquitoes and improved the writing of the manuscript. We thank Robert Johnston and Liz Urban for help with *in situs*. We also thank Greg Artiushin for the graphic designs created for the article. Studies outlined in this document were supported by grants from the National Institutes of Health, to C.J.P. (NIAID R01AI137078); the Department of Defense, to C.J.P. (W81XWH-17-PRMRP); and a Johns Hopkins Malaria Research Institute postdoctoral fellowship to S.E.M. We thank the Johns Hopkins Malaria Research Institute and Bloomberg Philanthropies for their support.

REFERENCES

Afify A, Betz J, Riabinina O, Lahondère C, and Potter C (2019). Commonly used insect repellents hide human odors from *Anopheles* mosquitoes. Curr. Biol 29, 3669–3680.e5. [PubMed: 31630950]

Athrey G, Cosme L, Popkin-Hall Z, Pathikonda W, and Slotman M (2017). Chemosensory gene expression in olfactory organs of the anthropophilic *Anopheles coluzzii* and zoophilic *Anopheles quadriannulatus*. BMC Genomics 18, 751. [PubMed: 28938869]

Basrur N, De Obaldia M, Morita T, Herre M, von Heynitz R, Tsitohay Y, and Vosshall L (2020). *Fruitless* mutant male mosquitoes gain attraction to human odor. Elife 9, e63982. [PubMed: 33284111]

Beauty B, and Marquardt W (1996). The Biology of Disease Vectors, First Edition (University Press of Colorado).

Bell J, and Wilson R (2016). Behavior reveals selective summation and max pooling among olfactory processing channels. Neuron 91, 425–438. [PubMed: 27373835]

Benton R, Sachse S, Michnick S, and Vosshall L (2006). Atypical membrane topology and heteromeric function of *Drosophila* odorant receptors in vivo. PLoS Biol. 4, e20. [PubMed: 16402857]

Bohbot J, Pitts R, Kwon H-W, Rützler M, Robertson H, and Zwiebel L (2007). Molecular characterization of the *Aedes aegypti* odorant receptor gene family. Insect Mol. Biol 16, 525–537. [PubMed: 17635615]

Bray N, Pimentel H, Melsted P, and Pachter L (2016). Near-optimzal probabilistic RNA-seq quantification. Nat. Biotechnol 34, 525–527. [PubMed: 27043002]

Butterwick J, Mármol J, Kim K, Kahlson M, Rogow J, Walz T, and Ruta V (2018). Cryo-EM structure of the insect olfactory receptor Orco. Nature 560, 447–452. [PubMed: 30111839]

Carey A, Wang G, Su C-Y, Zwiebel L, and Carlson J (2010). Odorant reception in the malaria mosquito *Anopheles gambiae*. Nature 464, 66–71. [PubMed: 20130575]

Chin S, Maguire S, Huoviala P, Jefferis G, and Potter C (2018). Olfactory neurons and brain centers directing oviposition decisions in *Drosophila*. Cell Rep. 24, 1667–1678. [PubMed: 30089274]

Clark J, and Ray A (2016). Olfactory mechanisms for discovery of odorants to reduce insect-host contact. J. Chem. Ecol 42, 919–930. [PubMed: 27628342]

Clowney E, LeGros M, Mosley C, Clowney F, Markenskoff-Papadimitriou C, Myllys M, Barnea G, Larabell C, and Lomvardas S (2012). Nuclear aggregation of olfactory receptor genes governs their monogenic expression. Cell 151, 724–737. [PubMed: 23141535]

Clyne P, Warr C, Freeman M, Lessing D, Kim J, and Carlson J (1999). A novel family of divergent seven-transmembrane proteins: candidate odorant receptors in *Drosophila*. Neuron 22, 327–338. [PubMed: 10069338]

Couto A, Alenius M, and Dickson B (2005). Molecular, anatomical, and functional organization of the Drosophila olfactory system. Curr. Biol 15, 1535–1547. [PubMed: 16139208]

Cowman A, Healer J, Marapana D, and Marsh K (2016). Malaria: biology and disease. Cell 167, 610–624. [PubMed: 27768886]

Dalton R, Lyons D, and Lomvardas S (2013). Co-opting the unfolded protein response to elicit olfactory receptor feedback. Cell 155, 321–332. [PubMed: 24120133]

DeGennaro M, McBride C, Seeholzer L, Nakagawa T, Dennis E, Goldman C, Jasinskiene N, James A, and Vosshall L (2013). *Orco* mutant mosquitoes lose strong preference for humans and are not repelled by volatile DEET. Nature 498, 487–491. [PubMed: 23719379]

Dobritsa A, van der Goes van Naters W, Warr C, Steinbrecht A, and Carlson J (2003). Integrating the molecular and cellular basis of odor coding in the *Drosophila* antenna. Neuron 37, 827–841. [PubMed: 12628173]

Elmore T, Ignell R, Carlson J, and Smith D (2003). Targeted mutation of a *Drosophila* odor receptor defines receptor requirement in a novel class of sensillum. J. Neurosci 23, 9906–9912. [PubMed: 14586020]

Feinstein P, Bozza T, Rodriguez I, Vassalli A, and Mombaerts P (2004). Axon guidance of mouse olfactory sensory neurons by odorant receptors and the β2 adrenergic receptor. Cell 117, 833–846. [PubMed: 15186782]

Foster W, and Takken W (2004). Nectar-related vs. human-related volatiles: behavioural response and choice by female and male *Anopheles gambiae* (Diptera:Culicidae) between emergence and first feeding. Bull. Entomol. Res 94, 145–157. [PubMed: 15153297]

German P, van der Poel S, Carraher C, Kralicek A, and Newcomb R (2013). Insights into subunit interactions within the insect olfactory receptor complex using FRET. Insect Biochem. Mol. Biol 43, 138–145. [PubMed: 23196131]

Ghaninia M, Hansson B, and Ignell R (2007). The antennal lobe of the African malaria mosquito, *Anopheles gambiae* - innervation and three-dimensional reconstruction. Arthropod Struct. Development 36, 23–39.

Giraldo-Calderón G, Emrich S, MacCallum R, Maslen G, Dialynas E, Topalis P, Ho N, Gesing S, Consortium V, Madey G, et al. (2015). Vector-Base: an updated bioinformatics resource for invertebrate vectors and other organisms related with human diseases. Nucleic Acids Res. 43, D707–D713. [PubMed: 25510499]

Global Malaria Programme (2019). World Malaria Report 2019 (WHO), p. 232.

Greppi C, Laursen W, Budelli G, Chang E, Daniels A, van Giesen L, Smidler A, Catteruccia F, and Garrity P (2020). Mosquito heat seeking is driven by an ancestral cooling receptor. Science 367, 681–684. [PubMed: 32029627]

Hallem E, Ho M, and Carlson J (2004). The molecular basis of odor coding in the Drosophila antenna. Cell 117, 965–979. [PubMed: 15210116]

Hamilton N, and Ferry M (2018). ggtern: ternary diagrams using ggplot2. J. Stat. Softw. Code Snippets 87, 1–17.

Hill C, Fox A, Pitts R, Kent L, Tan P, Chrystal M, Cravchik A, Collins F, Robertson H, and Zwiebel L (2002). G protein-coupled receptors in *Anopheles gambiae*. Science 298, 176–178. [PubMed: 12364795]

Hill S, Taparia T, and Ignell R (2021). Regulation of the antennal transcritome of the dengue vector, *Aedes aegyti*, during the first gonotropic cycle. BMC Genomics 22, 71. [PubMed: 33478394]

Jones P, Pask G, Rinker D, and Zwiebel L (2011). Functional agonism of insect odorant receptor ion channels. Proc. Natl. Acad. Sci. USA 108, 8821–8825. [PubMed: 21555561]

Karner T, Kellner I, Schultze A, Breer H, and Krieger J (2015). Co-expression of six tightly clustered odorant receptor genes in the antenna of the malaria mosquito *Anopheles gambiae*. Front. Ecol. Evol 3. 10.3389/fevo.2015.00026.

Konopka J, Task D, Afify A, Raji J, Deibel K, Maguire S, Lawrence R, and Potter C (2021). Olfaction in *Anopheles* mosquitoes. Chem. Senses 46, bjab021. [PubMed: 33885760]

Larsson M, Domingos A, Jones W, Chiappe M, Amrein H, and Vosshall L (2004). Or83b encodes a broadly expressed odorant receptor essential for Drosophila olfaction. Neuron 43, 703–714. [PubMed: 15339651]

Lewcock J, and Reed R (2004). A feedback mechanism regulates monoallelic odorant receptor expression. Proc. Natl. Acad. Sci. USA 101, 1069–1074. [PubMed: 14732684]

Lin C-C, and Potter C (2015). Re-classifcation of *Drosophila melanogaster* trichoid and intermediate sensilla using fluorescence-guided single sensillum recording. PLoS One 10, e0139675. [PubMed: 26431203]

McLaughlin C, Brbić M, Xiw Q, Li T, Horns F, Kolluru S, Kebschull J, Vacek D, Xie A, Li J, et al. (2021). Single-cell transcriptomes of developing and adult olfacotry receptor neurons in *Drosophila*. eLife 10, e63856. [PubMed: 33555999]

McMeniman C, Corfas R, Matthews B, Ritchie S, and Vosshall L (2014). Multimodal integration of carbon dioxide and other sensory cues drives mosquito attraction to humans. Cell 156, 1060–1071. [PubMed: 24581501]

Mombaerts P, Wang F, Dulac C, Chao S, Nemes A, Mendelsohn M, Edmondson J, and Axel R (1996). Visualizing an olfactory sensory map. Cell 87, 675–686. [PubMed: 8929536]

Montell C, and Zwiebel L (2016). Chapter ten - mosquito sensory systems. Adv. Insect Physiol 51, 293–328.

Mwingira V, Spitzen J, Mboera L, Torres-Estrada J, and Takken W (2019). The influence of larval stage and density on oviposition site-selection behavior of the Afrotropical malaria mosquito *Anopeles coluzzii* (Diptera: Culicidae). J. Med. Entomol 57, 657–666.

Mysore K, Flannery E, Tomchaney M, Severson D, and Duman-Scheel M (2013). Disruption of *Aedes aegypti* olfactory system development through Chitosan/siRNA nanoparticle targeting of *semaphorin-1a*. PLoS Negl. Trop. Dis 7, e2215. [PubMed: 23696908]

Mysore K, Flister S, Müller P, Rodrigues V, and Reichert H (2011). Brain development in the yellow fever mosquito *Aedes aegypti:* a comparative immunocytochemical analysis using cross-reacting antibodies from *Drosophila melanogaster*. Developmental Genes Evol. 221, 281–296.

Neuhaus E, Gisselmann G, Zhang W, Dooley R, Störtkuhl K, and Hatt H (2005). Odorant receptor heterodimerization in the olfactory system of *Drosophila melanogaster*. Nat. Neurosci 8, 15–17. [PubMed: 15592462]

Omondi A, Ghaninia M, Dawit M, Svensson T, and Ignell R (2019). Age-dependent regulation of host seeking in *Anopheles coluzzii*. Scientific Rep. 9, 9699.

Pfeiffer B, Ngo T-T, Hibbard K, Murphy C, Jenett A, Truman J, and Rubin G (2010). Refinement of tools for targeted gene expression in Drosophila. Genetics 186, 735–755. [PubMed: 20697123]

Pimentel H, Bray N, Puente S, Melsted P, and Pachter L (2017). Differential analysis of RNA-Seq incorporating quantification uncertainty. Nat. Methods 14, 687–690. [PubMed: 28581496]

Pitts R, Rinker D, Jones P, Rokas A, and Zwiebel L (2011). Transcriptome profiling of chemosensory appendages in the malaria vector *Anopheles gambiae* reveals tissue- and sex-specific signatures of odor coding. BMC Genomics 12, 271. [PubMed: 21619637]

Potter C, and Luo L (2010). Splinkerette PCR for mapping transposable elements in *Drosophila*. PLoS One 5, e10168. [PubMed: 20405015]

R Core Team (2018). R: A Language and Environment for Statistical Computing (R Foundation for Statistical Computing).

Raji J, Melo N, Castillo J, Gonzalez S, Saldana V, Stensmyr M, and DeGennaro M (2019). *Aedes aegypti* mosquitoes detect acidic volatiles found in human odor using the IR8a pathway. Curr. Biol 29, 1253–1262. [PubMed: 30930038]

Ray A, van der Goes van Naters W, Shiraiwa T, and Carlson J (2007). Mechanisms of odor receptor gene choice in *Drosophila*. Neuron 53, 353–369. [PubMed: 17270733]

Riabinina O, Luginbuhl D, Marr E, Liu S, Wu M, Luo L, and Potter C (2015). Improved and expanded Q-system reagents for genetic manipulations. Nat. Methods 12, 219–222. [PubMed: 25581800]

Riabinina O, Task D, Marr E, Lin C-C, Alford R, O'Brochta D, and Potter C (2016). Organization of olfactory centers in the malaria mosquito *Anopheles gambiae*. Nat. Commun 7, 13010. [PubMed: 27694947]

Schindelin J, Arganda-Carreras I, Frise E, Kaynig V, Longair M, Pietzsch T, Preibisch S, Rueden C, Saalfeld S, Schmid B, et al. (2012). Fiji: an open-source platform for biological-image analysis. Nat. Methods 9, 676–682. [PubMed: 22743772]

Serizawa S, Miyamichi K, Nakatani H, Suzuki M, Saito M, Yoshihara Y, and Sakano H (2003). Negative feedback regulation ensures the one receptor-one olfactory neuron rule in mouse. Science 302, 2088–2094. [PubMed: 14593185]

Shykind B, Rohani S, O'Donnell S, Nemes A, Mendelsohn M, Sun A, Axel R, and Barnea G (2004). Gene switching and the stability of odorant receptor gene choice. Cell 117, 801–815. [PubMed: 15186780]

Sullivan S, Adamson M, Ressler K, Kozak C, and Buck L (1996). The chromosomal distribution of mouse odorant receptor genes. Proc. Natl. Acad. Sci. USA 93, 884–888. [PubMed: 8570653]

Sun H, Liu F, Ye Z, Baker A, and Zwiebel L (2020). Mutagenesis of the orco odorant receptor co-receptor impairs olfactory function in the malaria vector *Anopheles coluzzii*. Insect Biochem. Mol. Biol 127, 103497. [PubMed: 33188923]

Sweeney L, Couto A, Chou Y, Berdnik D, Dickson B, Luo L, and Komiyama T (2007). Temporal target restriction of olfactory receptor neurons by Semaphorin-1a/PlexinA-mediated axon-axon interactions. Neuron 53, 185–200. [PubMed: 17224402]

Tallon A, Hill S, and Ignell R (2019). Sex and age modulate antennal chemosensory-related genes linked to the onset of host seeking in the yellow-fever mosquito, *Aedes aegypti*. Scientific Rep. 9, 43.

The R Development Core Team (2018). R: A Language and Environment for Statistical Computing (R Foundation for Statistical Computing).

Trebels B, Dippel S, Goetz B, Graebner M, Hofmann C, Hofmann F, Schmid F-R, Uhl M, YVuong M-P, Weber V, et al. (2021). Metamorphic development of the olfactory system in the red flour beetle (*Trobolium castaneum, HERBST*. BMC Biol. 19, 1–18. [PubMed: 33407428]

Tsitoura P, Andronopoulou E, Tsikou D, Agalou A, Papakonstantinou M, Kotzia G, Labropoulou V, Swevers L, Georgoussi Z, and Iatrou K (2010). Expression and membrane topology of *Anopheles gambiae* odorant receptors in Lepidopteran Insect Cells. PLoS One 5, e15428. [PubMed: 21082026]

Vassar R, Chao S, Sitcheran R, Nuñez J, Vosshall L, and Axel R (1994). Topographic organization of sensory projections to the olfactory bulb. Cell 79, 981–991. [PubMed: 8001145]

Wang F, Nemes A, Mendelsohn M, and Axel R (1998). Odorant receptors govern the formation of a precise topographic map. Cell 93, 47–60. [PubMed: 9546391]

Younger M, Herre M, Ehrlich A, Gong Z, Gilbert Z, Rahiel S, Matthews B, and Vosshall L (2020). Non-canonical odor coding ensures unbreakable mosquito attraction to humans. Preprint at bioRxiv. 10.1101/2020.11.07.368720.

Zhang X, Rodriguez I, Mombaerts P, and Firestein S (2004). Odorant and vomeronasal receptor genes in two mouse genome assemblies. Genomics 83, 802–811. [PubMed: 15081110]

Highlights

- Ectopic OR expression disrupts mosquito olfactory neuron activity
- Expression of an OR in mosquitoes reduces endogenous OR expression
- Onset of mosquito OR expression extends into adult stages
- Mosquitoes host seek despite the lack of OR neuron function

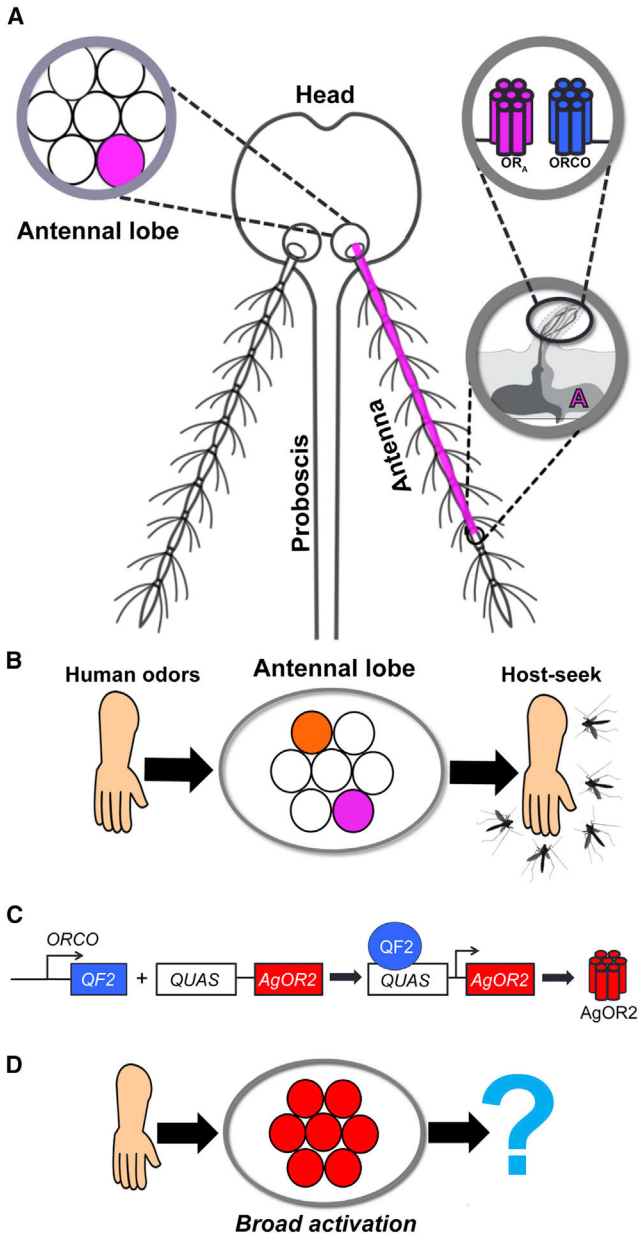

Figure 1. Strategy to manipulate the olfactory system of *Anopheles* mosquitoes

(A) Anatomy of OR-guided olfaction. Mosquitoes smell odors in the environment using 3 olfactory organs: the proboscis, the maxillary palps (not shown), and the antennae. A single antenna is made up of 13 segments called flagellomeres. Each flagellomere is covered with sensory hairs called sensilla, a single one of which houses up to 4 ORNs. An ORN expresses 1 of 3 chemosensory gene families: the *IRs*, the *GRs*, or the *ORs*. The *OR* gene family plays an important role in host-seeking behavior. There are 75 different ORs in the *Anopheles gambiae* genome, each of which is sensitive to specific odorants in the environment. Only 1 OR (OR_A) is expressed per ORN (encircled A). At the dendrites of ORN A, OR*A* couples with ORCO. When odorants bind to OR_A-ORCO complexes, ORN A becomes active and

sends its excitatory signal down its axon, targeting a discrete brain region of the mosquito AL called a glomerulus (shown as a pink circle).

(B) A human-specific odor code in the mosquito brain. Human odorants bind to specific ORs, activating the ORNs on which they are expressed. Activated ORNs target discrete glomeruli (pink, orange) in the AL to guide host seeking.

(C) Olfactogenetics strategy. Using the Q-system, the *ORCO-QF2* transgene (Riabinina et al., 2016) was combined with the effector construct *QUAS-AgOR2*. The combination of these transgenes causes AgOR2 to be expressed in $ORCO^{+}$ ORNs.

(D) Test of the olfactogenetics strategy. AgOR2 responds to major components of human and animal odors such as indole and benzaldehyde. We hypothesized that *ORCO > AgOR2* mosquitoes would experience broad activation of the majority of the AL in the presence of a human, thereby dysregulating the human-specific odor code in the mosquito brain (Figure 1B). *ORCO > AgOR2* mosquitoes would then be evaluated for reduced host-seeking behavior.

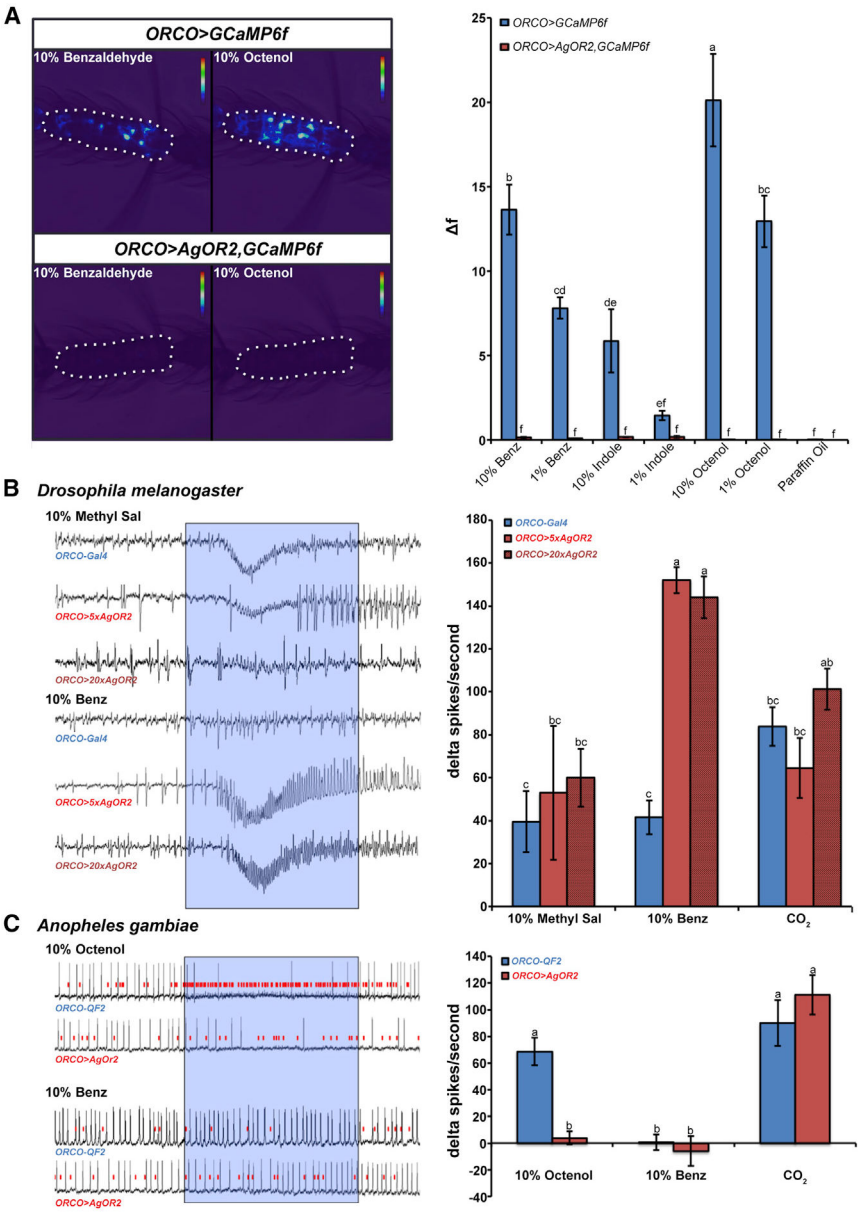

Figure 2. Olfactogenetics impairs *Anopheles* but not *Drosophila ORCO*$^{+}$ ORNs

(A) *ORCO > AgOR2,GCamp6f* mosquitoes show impaired olfactory responses to human odorants. The activity of ORNs in antennal segment 11 (outlined with a white dotted line) was detected by calcium imaging of *ORCO*$^{+}$ neurons expressing *GCaMP6f* (Afify et al., 2019). Relative to controls (*ORCO > GCaMP6f*), mosquito antennal segments with the ectopic expression of *AgOR2* and *GCaMP6f (ORCO > AgOR2,GCaMP6f)* show impaired responses to benzaldehyde (10% and 1%) and indole (10%), the cognate ligands of AgOR2. They also show dampened responses to octenol (10% and 1%). A 2-way repeated measures ANOVA was conducted to test the effect of odorant and genotype on calcium responses ($F(6,7) = 75.1$, $p < 0.001$). Groups with different letter values (A–F) are statistically different as determined by the Tukey post hoc honest significant difference (HSD) test. Each sample

included in the analysis was taken from a different female mosquito. $n_{ORCO>GCaMP6f} = 9$, $n_{ORCO>AgOR2,GCaMP6f} = 8$.

(B) Ectopic expression of *AgOR2* in *Drosophila* ab1 sensilla does not impair ORN physiology. The cognate ligand of DmOR10a-expressing neurons is methyl salicylate (Methyl Sal). Driving *AgOR2* into this neuronal group using the *5xUAS* or *20xUAS* effector lines does not affect the response of DmOR10a to Methyl Sal. *ORCO*$^+$ ORNs of *ORCO > 5xAgOR2* and *ORCO > 20xAgOR2* animals show an ectopic response to benzaldehyde (Benz). The presence of the *ORCO*$^-$ CO_2 neuron was used to verify that recordings were taken from the ab1 sensillum. The activity of the CO_2 neuron is not affected by the experimental manipulation. Odorant or CO_2 stimulus was delivered in the time frame denoted by the blue translucent box. A 2-way repeated measures ANOVA was used to determine the significance of genotype and odorant on delta spikes/s ($F(4,28) = 13.7$, $p < 0.0001$). Groups with different letter values (A-C) are statistically different as determined by the Tukey post hoc HSD test. Two to three females per genotype were analyzed. The number of sensilla evaluated for each group was $n_{ORCO\text{-}GAL4} = 9$; $n_{ORCO>5xAgOR2} = 4$; $n_{ORCO>20xAgOR2} = 5$.

(C) Olfactogenetics impairs *ORCO*$^+$ ORN physiology in *Anopheles*. SSR from the *Anopheles* maxillary palp cp sensilla. The cognate ligand of AgOR8-expressing neurons is octenol. Driving *AgOR2* into this neuron group interferes with the response of AgOR8 to octenol (smallest spiking neurons; red lines indicate AgOR8 activity). The ORNs ectopically expressing *AgOR2* do not respond to Benz. The presence of the *ORCO*$^-$ CO_2 neuron was used to verify that recordings were taken from a cp sensillum. The activity of the CO_2 neuron was not affected by the experimental manipulation. Odorant or CO_2 was delivered in the time frame denoted by the blue translucent box. A 2-way repeated measures ANOVA was used to determine that there was a significant effect at odorant and genotype on delta spikes/s ($F(4,5) = 8.5$, $p = 0.01$). Groups with different letter values (A and B) are statistically different as determined by the Tukey post doc HSD test. Two to three females per genotype were analyzed. The number of sensilla evaluated for each group was $n_{ORCO\text{-}QF2} = 6$; $n_{ORCO>AgOR2} = 5$. The error bars in all of the quantified figures represent the standard error of the mean (SEM).

For (B and C) (left), the x axis represents time (ms) and the y axis represents voltage.

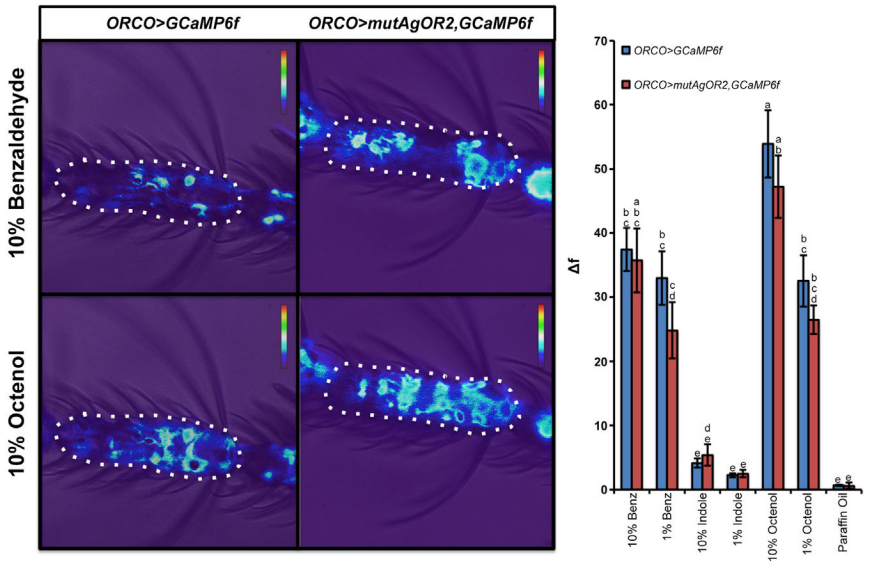

Figure 3. AgOR2 protein is required for the dominant-negative olfactory phenotype caused by *ORCO > AgOR2* expression

The *mutAgOR2* transgene contains an introduced point mutation in the start codon of *AgOR2* and a frameshift mutation at a second in-frame ATG site of the gene. Odorant-evoked responses (Δf) were calculated from the 11th segment of the mosquito antennae (outlined with dotted lines). Representative control and experimental calcium imaging responses to 10% Benz and 10% octenol are shown. Antennae from *ORCO > mutAgOR2,GCaMP6f* mosquitoes show no difference in responses to odorants from control (*ORCO > GCaMP6f*). A 2-way repeated measures ANOVA was used to determine whether there was a significant effect of odorant and genotype on calcium responses ($F(6,9) = 47.3$, $p < 0.0001$). Groups with different letter values (a–d) are statistically different as determined by the Tukey post hoc HSD test. The error bars represent SEMs. Each sample included in the analysis was taken from a different female mosquito. $n_{ORCO>GCaMP6f} = 11$, $n_{ORCO>mutAgOR2,GCaMP6f} = 5$.

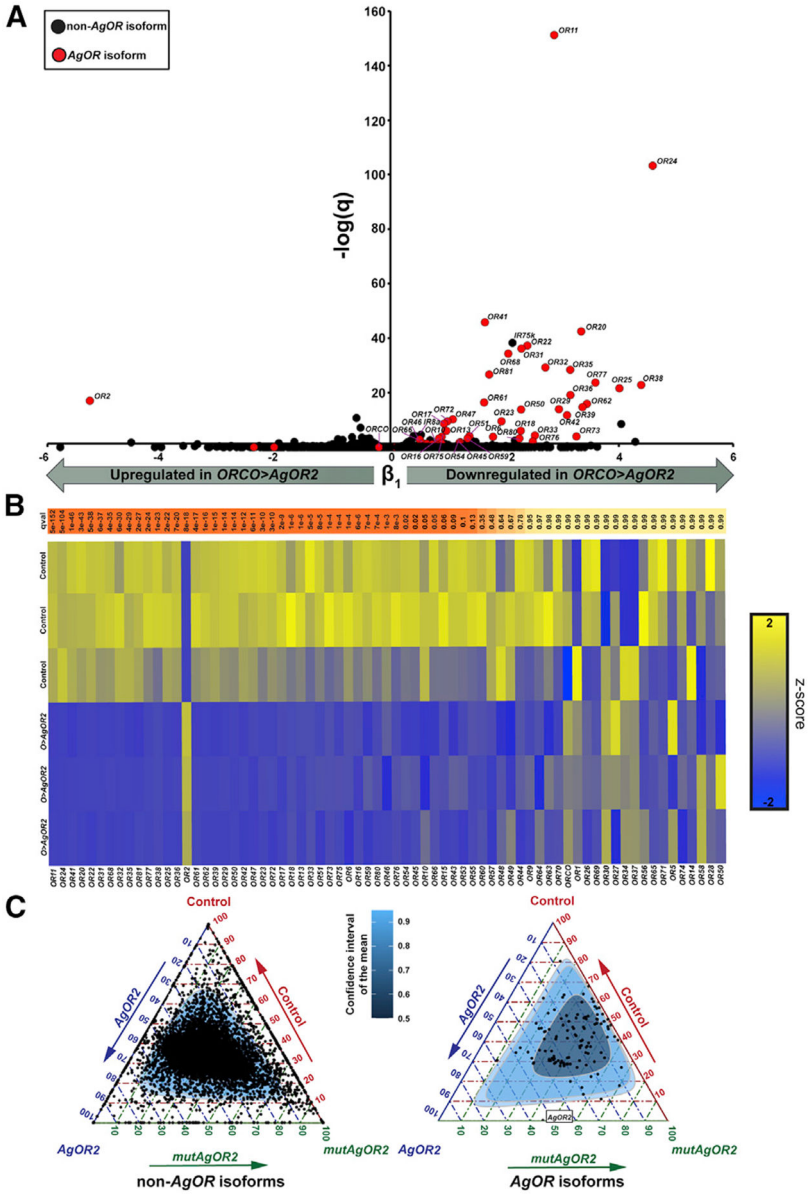

Figure 4. Ectopic AgOR2 protein reduces the transcript levels of *AgOR* isoforms

(A) Volcano plot of differentially expressed isoforms. Using Wald tests, we evaluated whether the 13,224 isoforms present in 3 triplicates of control and 3 triplicates of *ORCO > AgOR2* antennae (~200 antennae per sample) were differentially expressed. Non-*A. gambiae OR* and *A. gambiae OR* isoforms are shown as black or red dots, respectively. Only 0.63% of the transcriptome is differentially regulated in *ORCO > AgOR2*, in which 49% of those transcripts are *AgORs* (Figure S6; Data S2). log(q) is the level of significance of β_1, which, for each isoform, is defined as $TPM_{control} - TPM_{experimental}$. The 41 *AgORs* found to be significant from the Wald tests are labeled according to their gene annotation in the volcano plot. *AgORCO*, while not differentially expressed, is also indicated on the plot. All *AgORs* (with the exception of *AgOR2*) that are differentially expressed are downregulated in the experimental condition when compared to wild type. Interestingly, *AgIR8a* and

AgIR75k (indicated on the volcano plot) are downregulated in *ORCO > AgOR2*. The remaining *AgIRs* and *AgGRs* are unaffected.

(B and C) Heatmap of the *AgOR* gene family. A *Z* score was computed for each cell in the heatmap by subtracting the mean isoform TPM from the TPM of the cell divided by the standard deviation (SD) of the isoform TPM. *AgORs* are sorted along the x axis according to their significance level (q value) from the Wald tests in (A) Darker orange is most significant and yellow is not significant. Note that *ORCO > AgOR2* is listed as *O > AgOR2*. (C) Ectopic AgOR2 protein is required for the observed downregulation of native *AgOR* transcripts. Ternary plots were used to visualize the relative ratio of a genotype to the relative abundance level of an isoform using the formula $(TPM_{genotypex})/(\text{mean } TPM_{control} + \text{mean } TPM_{ORCO>AgOR2} + \text{mean } TPM_{ORCO>mutAgOR2}) \times 100$. There are equal ratios of transcript abundance levels for non-*AgOR* genes among the 3 genotypes (left). However, the relative contribution to transcript abundance levels of control, *ORCO > AgOR2*, and *ORCO > mutAgOR2* are skewed in the *AgOR* gene family such that *AgOR* gene levels in *ORCO > mutAgOR2* and control are relatively similar and higher than *ORCO > AgOR2* levels, with the exception of *AgOR2* itself (whose abundance is similar between *ORCO > AgOR2* and *ORCO > mutAgOR2*) (right).

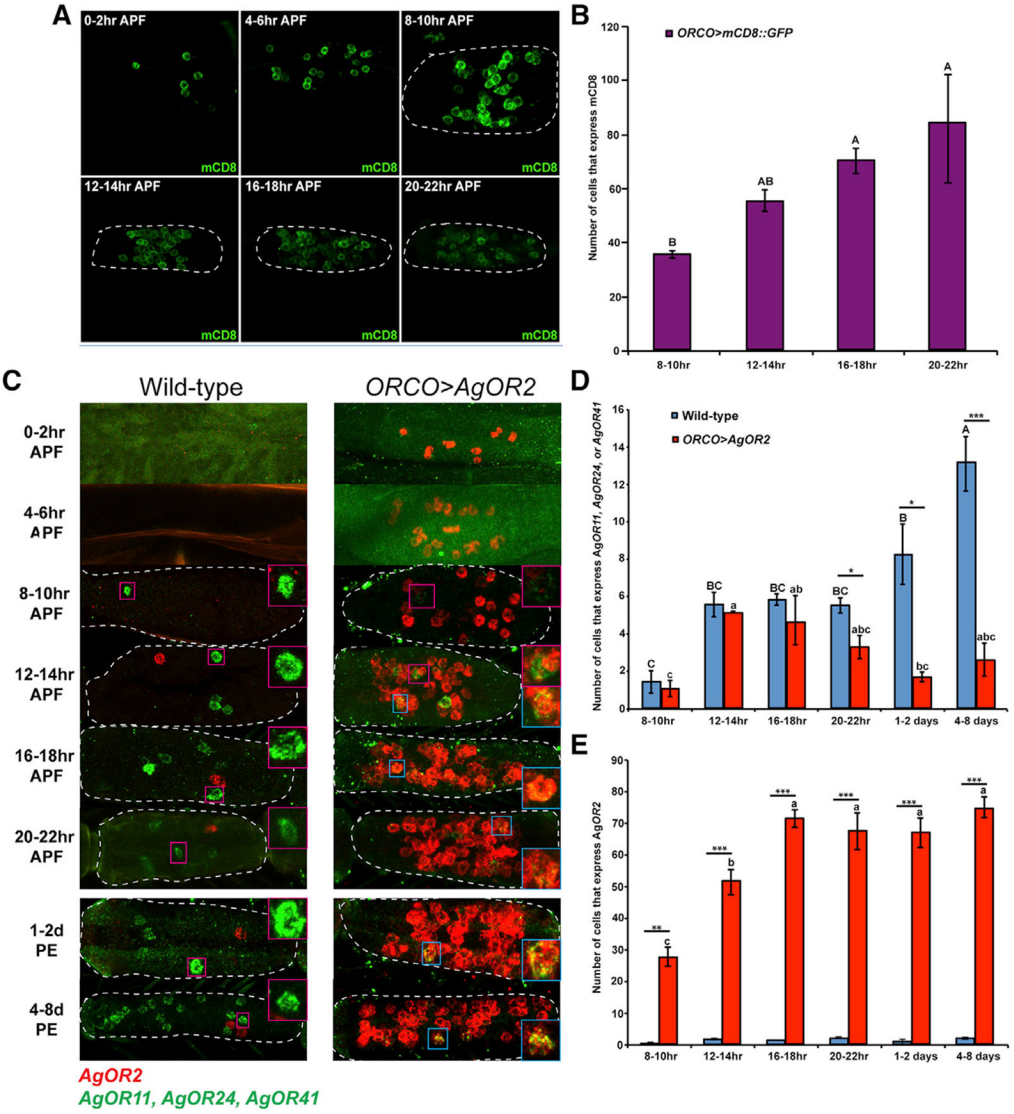

Figure 5. AgOR2-feedback occurs during the adult stage

(A) AgORCO is expressed at the start of pupal ecdysis. Representative immunohistochemistry images of ORCO-expressing neurons in the *ORCO > mCD8:GFP* genotype. Pupal antennae were extracted at the indicated time point and stained with anti-mCD8 (green). Cells were scored as ORCO^{+} based on the presence of mCD8.

(B) ORCO^{+} cell number increases over pupal development. An ANOVA was used to determine whether the number of cells that express mCD8 change over pupal development. There was a significant effect of time on the number of cells that express mCD8 ($F(3,16) = 6.44$, $p = 0.0046$). Groups with different letter values are statistically different as determined by the Tukey post hoc HSD test (A and B).

(C–E) Representative *in situ* hybridization images of wild-type and *ORCO > AgOR2* antennae hybridized to probes against *AgOR2* (red) and *AgOR11, AgOR24, AgOR41* (green) mRNA. Tissue was sampled every 4 h APF as well as 1–2 days PE and 4–8 days PE. The pink insets (top right) of each panel show *AgOR11, AgOR24, AgOR41*-expressing

cells without *AgOR2* co-expression and the blue insets (bottom right) show cells with co-expression. *AgOR2* did not co-express with *AgOR11, AgOR24, AgOR41* in wild-type ORNs. Independent sample t tests were conducted to compare the number of cells that express *AgOR11, AgOR24*, and *AgOR41* (D) or *AgOR2* (E) between wild type and *ORCO > AgOR2* for each time point. *$p < 0.05$, **$p < 0.005$, ***$p < 0.0005$. For the results of each statistical test, refer to Table S1. An ANOVA was used to determine whether the number of cells that express *AgOR11, AgOR24*, and *AgOR41* (D) or (E) *AgOR2* change within the given genotype over time. There was a significant effect of time on the number of cells that express *AgOR11, AgOR24*, and *AgOR41* in wild type ($F(5,24) = 15.8$, $p < 0.0001$) and *ORCO > AgOR2* ($F(5,22) = 4.54$, $p = 0.005$) flagellomeres and the number of cells that express *AgOR2* in *ORCO > AgOR2* ($F(5,22 = 26.7$, $p < 0.0001$). There was no effect of time of the number of cells that express *AgOR2* in wild-type flagellomeres. For both immunochemistry and *in situ* hybridization experiments, cells were scored once per flagellomere (after 8–10 h APF, inclusive). For each time point, cells from 1 flagellomere per animal in an average of 5 animals per time point were scored. The location of each scored flagellomere was randomized for each antenna.

Flagellomeres in (A and C) are indicated by a dotted white line. The error bars in (C–E) represent SEMs.

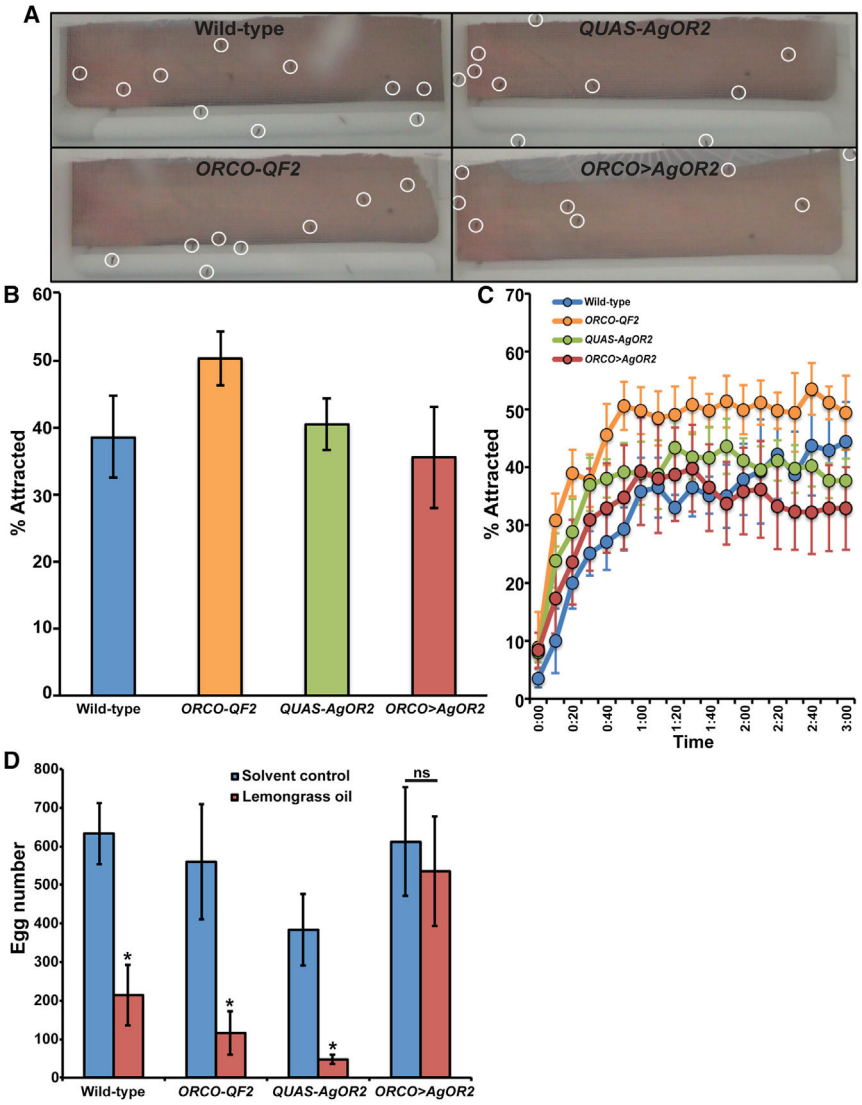

Figure 6. *ORCO > AgOR2* mosquitoes remain attracted to a human host

(A) Representative images of wild-type, *ORCO-QF2, QUAS-AgOR2*, and *ORCO > AgOR2* mosquitoes (circled) in the host-proximity assay. Mosquitoes attracted to an arm (2.5 cm from the cage) that land on the net are counted.

(B) Results of the host-proximity assay. A 1-way ANOVA between subjects was conducted to compare the effect of genotype on percentage of attraction. There was no effect of genotype on percentage of attraction at the $p < 0.05$ level for the 4 groups ($F(3) = 1.08$, $p = 0.37$). A total of 20–30 female mosquitoes were tested per trial. The number of trials per genotype: $n_{\text{wild-type}} = 5$; $n_{ORCO\text{-}QF2} = 5$; $n_{QUAS\text{-}AgOR2} = 7$; $n_{ORCO>AgOR2} = 7$.

(C) Time course of mosquito attraction toward a human host by genotype. Over the course of 3 min, there was no difference in the percentage of mosquitoes attracted to a human host.

(D) Results of the olfactory-based oviposition preference assay. Paired-samples t tests were conducted to compare the total number of eggs laid in solvent control double cups and in lemongrass oil (0.1%) double cups for each genotype (wild type, *ORCO-QF2, QUAS-AgOR2*, and *ORCO > AgOR2*). Control genotypes (wild type, *ORCO-QF2*, and

QUAS-AgOR2) laid fewer eggs in lemongrass oil than the solvent control double cups (wild type: solvent control [mean = 632.4, SD = 208.5] and lemongrass oil [mean = 213, SD = 207.7], t(6) = 2.8, p < 0.05; *ORCO-QF2*: solvent control [mean = 560.1, SD = 394.9] and lemongrass oil [mean = 116.1, SD = 151.9], t(6) = 2.8, p < 0.05; *QUAS-AgOR2*: solvent control (mean = 384.3, SD = 246.4] and lemongrass oil [mean = 47.7, SD = 31.6], t(6) = 3.4, p < 0.05]). *ORCO > AgOR2* mosquitoes laid the same number of eggs in solvent (mean = 612, SD = 374) and lemongrass oil (mean = 535.7,SD = 376.8), t(6) = 0.34, p = 0.74 double cups. ns, not significant, *p < 0.05. The number of trials per genotype: $n_{\text{wild-type}}$ = 7; $n_{ORCO\text{-}QF2}$ = 7; $n_{QUAS\text{-}AgOR2}$ = 7; $n_{ORCO>AgOR2}$ = 7. The error bars in (B–D) represent SEMs.

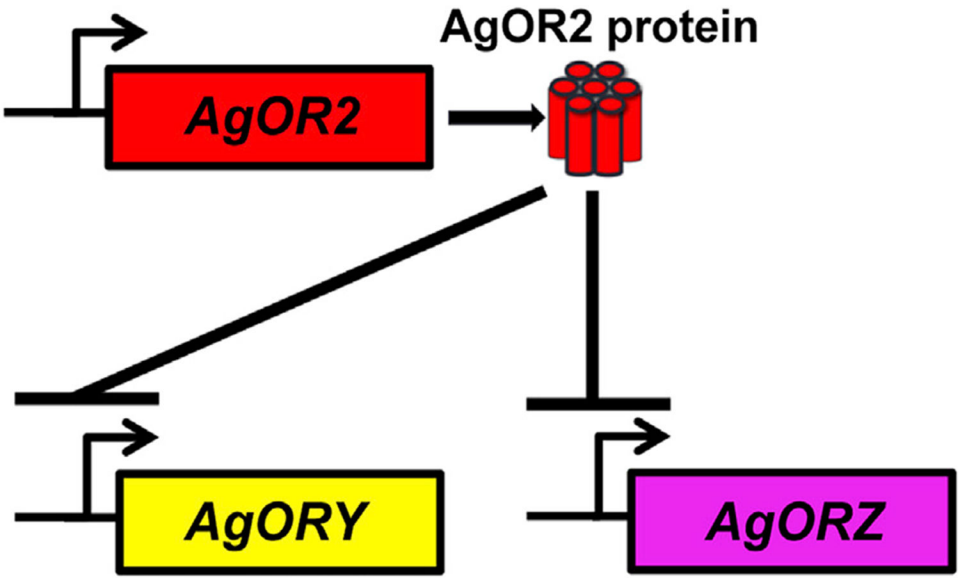

Figure 7. Summary model

Ectopic AgOR2 negatively regulates the expression of *AgOR* transcripts. Our data implicate a mechanism of negative regulation of most of the *AgOR* transcripts (e.g., *AgORY, AgORZ*) by ectopic AgOR2 protein.

KEY RESOURCES TABLE

REAGENT or RESOURCE	SOURCE	IDENTIFIER
Antibodies		
Mouse anti-*Apocrypta bakeri* ORCO	(Butterwick et al., 2018)	#15B2
Rat anti-CD8	Invitrogen	Cat#MCD0800; RRID:AB_10392843
Mouse anti-nc82	Developmental Studies Hybridoma Bank	RRID: AB_2392664
Alexa-488 goat anti-rat	Invitrogen	Cat#A110066
Chemicals, peptides, and recombinant proteins		
Benzaldehyde	Millipore Sigma	B1334; CAS: 100-52-7
Methyl Salicylate	Millipore Sigma	M6752; CAS: 119-36-8
Lemongrass oil	Millipore Sigma	W262440; CAS: 8007-02-01
Critical commercial assays		
In-Fusion HD Cloning System	Clontech	639645
Midiprep kit	Qiagen	12145
Deposited data		
Raw and analyzed RNA-seq data	This paper	BioProject: PRJNA771697
Experimental models: Organisms/strains		
An. coluzzii: ORCO-QF2	(Riabinina et al., 2016)	BEI Resources:MRA-1300
An. coluzzii: QUAS-mCD8::GFP	(Riabinina et al., 2016)	BEI Resources:MRA-1301
An. coluzzii: QUAS-GCaMP6f	(Afify et al., 2019)	N/A
An. coluzzii: Wild-type M-form strain Ngousso	Insect Transformation Facility (Rockville, MD)	N/A
D. melanogaster: ORCO-GAL4; P{Orco-GAL4.W}11.17	Bloomington Drosophila Stock Center	BDSC: 26818
D. melanogaster: 5xUAS-AgOR2; w[*];Df(2L)dp-79b Dp(2;2)dpp[d21]/cyo; P{w[+mC]=UAS-Agam\Or2}3/TM3,Sb[1]	Bloomington Drosophila Stock Center	BDSC: 58828
D. melanogaster: Pebbled-GAL4; w[*]P{w[+m]=GAL4}peb*	Bloomington Drosophila Stock Center	BDSC: 80570
An. coluzzii: QUAS-AgOR2	This paper	N/A
An. coluzzii: QUAS-mutAgOR2	This paper	N/A
D. melanogaster: 20xUAS-AgOR2	This paper	N/A
Oligonucleotides		
Aga_OR2_F: ATTCGTTAACAGATCTAT GCTGATCGAAGAGTGTCCGA	This paper	N/A
Aga_OR2_R: CCTTCACAAAGATCGAC GTCTTAGTTGTACACTCGGCGCAGC	This paper	N/A
InfuMUTAgOr2_for: ATTCGTTAACAGATCTTTTC TGATCGAAGAGTGTCCGATAATTG	This paper	N/A
InfuMUTAGOr2_rev: CGTCATTTTTCTCGAGTA GAGAGCGTACTCGGCGGC	This paper	N/A
UAS-AgOr2-FOR: TTACTTCAGGCGGCC GCAAA ATGCTGATCGAAGAGTGTCCG	This paper	N/A
UAS-AgOR2-REV: ACAAAGATCCTCTAGA TTAGTTGTACACTCGGCGCAG	This paper	N/A
gcamp6f_for2: ATGGTATGGCTAGCATGACTG	This paper	N/A

REAGENT or RESOURCE	SOURCE	IDENTIFIER
gcamp6f_rev: GTAGTTTACCTGACCATCCCC	This paper	N/A
AgOr2_for1: TAATTGGTGTCAATGTGCGAG	This paper	N/A
AgOr2_rev2: TTATCGGCTCCTCAAAGTCTG	This paper	N/A
Recombinant DNA		
pXL-BacII-15xQUAS-TATA-AgOR2-Sv40	This paper	N/A
pXL-BacII-15xQUAS_TATA-Sv40	(Riabinina et al., 2016)	Addgene Plasmid #104875
pXL-BacII-15xQUAS-TATA-mutAgOR2-Sv40	This paper	N/A
pJFRC-20xUAS-AgOR2	This paper	N/A
pJFRC-20xUAS-IVS-CD8GFP	(Pfeiffer et al., 2010)	Addgene Plasmid #26220
pXL-BACII-DsRed-OR7_9kbProm-QF2-hsp70	(Riabinina et al., 2016)	Addgene Plasmid #104877
Software and algorithms		
MacVector v17.0.10	MacVector, Inc.	Macvector.com
Fiji software	(Schindelin et al., 2012)	imagej.net
JMP Version 9	SAS Institute, Inc	jmp.com
AUTOSPIKE software	USB-IDAC System; Syntech	ockenfels-syntech.com
Kallisto v0.46.0	(Bray et al., 2016)	N/A
R	(The R Development Core Team and Computing, 2018)	r-project.org
Sleuth v0.30.0	(Pimentel et al., 2017)	rdocumentation.org
Ggtern R package	(Hamilton and Ferry, 2018)	cran.r-project.org
Other		
Company used for *D. melanogaster* transformation	Rainbow Transgenics	rainbowgene.com
Company used for *An. coluzzii* transformation	The Insect Transformation Facility	ibbr.umd.edu/facilities/itf
Company used for RNA-seq library preparation and sequencing	Genewiz, Inc.	genewiz.com
Company used to construct RNA probes	Molecular instruments	molecularinstruments.com